Connecting *GCN5*'s centromeric SAGA to the mitotic tension-sensing checkpoint

Emily L. Petty, Masha Evpak, and Lorraine Pillus*
Division of Biological Sciences, Molecular Biology, UCSD Moores Cancer Center, University of California, San Diego, La Jolla, CA 92103

ABSTRACT **Multiple interdependent mechanisms ensure faithful segregation of chromosomes during cell division. Among these, the spindle assembly checkpoint monitors attachment of spindle microtubules to the centromere of each chromosome, whereas the tension-sensing checkpoint monitors the opposing forces between sister chromatid centromeres for proper biorientation. We report here a new function for the deeply conserved Gcn5 acetyltransferase in the centromeric localization of Rts1, a key player in the tension-sensing checkpoint. Rts1 is a regulatory component of protein phopshatase 2A, a near universal phosphatase complex, which is recruited to centromeres by the Shugoshin (Sgo) checkpoint component under low-tension conditions to maintain sister chromatid cohesion. We report that loss of Gcn5 disrupts centromeric localization of Rts1. Increased *RTS1* dosage robustly suppresses *gcn5*Δ cell cycle and chromosome segregation defects, including restoration of Rts1 to centromeres. Sgo1's Rts1-binding function also plays a key role in *RTS1* dosage suppression of *gcn5*Δ phenotypes. Notably, we have identified residues of the centromere histone H3 variant Cse4 that function in these chromosome segregation-related roles of *RTS1*. Together, these findings expand the understanding of the mechanistic roles of Gcn5 and Cse4 in chromosome segregation.**

Monitoring Editor
Yukiko Yamashita
University of Michigan

Received: Dec 6, 2017
Revised: Jun 29, 2018
Accepted: Jul 2, 2018

INTRODUCTION

The eukaryotic genome is packaged into the DNA–protein complex defined as chromatin. This packaging is dynamic, ensuring that cells can make rapid alterations to gene expression, respond to DNA damage, and divide their genomes accurately. As its foundation, chromatin is made up of nucleosomes, the repeated units of DNA wrapped around octamers of histone proteins (Kornberg and Lorch, 1999). Multiple, diverse enzymes add small and large chemical groups or proteins to histone residues and opposing enzymes remove these modifications, contributing to the dynamic nature of chromatin organization necessary for life and growth in an ever-changing environment (Tessarz and Kouzarides, 2014).

Gcn5 is one enzyme that adds the small acetyl group to histones H3 and H2B within chromatin and other substrates as well (Grant *et al.*, 1997, 1999; Downey *et al.*, 2015). There are three biochemically distinct, multisubunit complexes that contain Gcn5 in yeast. Among these, SAGA (Spt-Ada-Gcn5 acetyltransferase) and SLIK/SALSA (SAGA-Like/SAGA altered Spt8 absent) are large cotranscriptional activator complexes that target H3K9 and K14 acetylation near gene promoters (Grant *et al.*, 1997; Roberts and Winston, 1997; Pray-Grant *et al.*, 2002; Sterner, Belotserkovskaya, and Berger, 2002; Rosaleny, Ruiz-Garcia, *et al.*, 2007). The smaller ADA complex may contribute to broad H3 acetylation outside promoters (Eberharter *et al.*, 1999; Lee, Sardiu, *et al.*, 2011). Characterization of *gcn5*Δ mutants in yeast revealed late cell cycle delays and mitotic errors pointing to roles in chromosome segregation (Zhang *et al.*, 1998; Howe *et al.*, 2001; Vernarecci *et al.*, 2008). Gcn5 also contributes to chromatin organization in centromeric regions (Vernarecci *et al.*, 2008) and regulates a tension-sensing function of H3 during chromosome segregation (Luo, Deng, *et al.*, 2016).

Successful chromosome segregation begins with genomic replication, followed by massive condensation of interphase chromatin into chromatids, and sister chromatid pairing. Sister chromatids remain paired at their centromeres, encircled by the multimeric cohesin ring complex, until all chromosomes are aligned and attached to

This article was published online ahead of print in MBoC in Press (http://www.molbiolcell.org/cgi/doi/10.1091/mbc.E17-12-0701) on July 11, 2018.

*Address correspondence to: Lorraine Pillus (lpillus@ucsd.edu).

Abbreviations used: 5-FOA, 5-fluoroorotic acid; HU, hydroxyurea; MMS, methyl methanesulfanate; NOC, nocodazole; SAC, spindle assembly checkpoint; SAGA, Spt-Ada-Gcn5 acetyltransferase complex; SALSA, SAGA altered, Spt8 absent; SLIK, SAGA-Like complex.

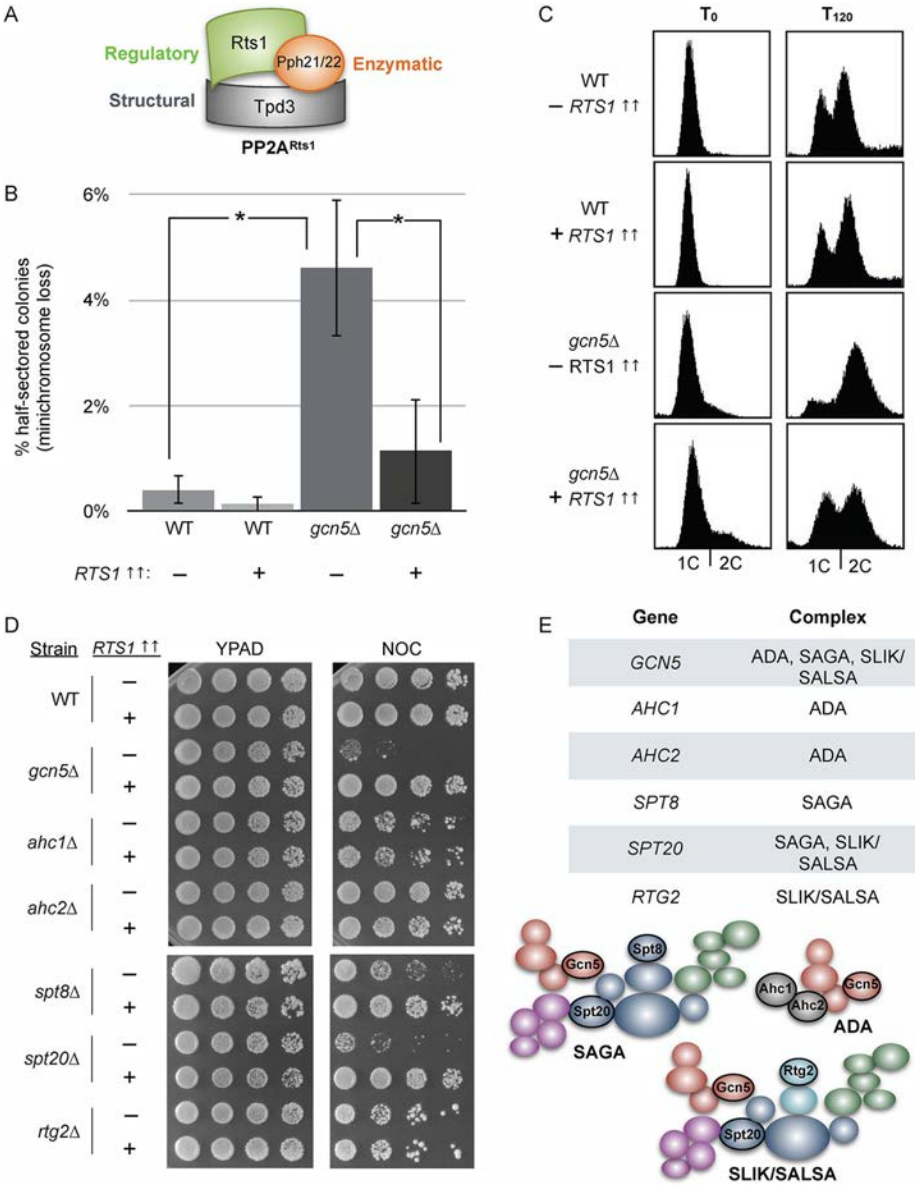

FIGURE 1: Overexpression of *RTS1* rescues late cell cycle and chromosome segregation-related *gcn5*Δ phenotypes. (A) Rts1 is the regulatory subunit of the PP2A-Rts1 complex, which is functionally linked to Gcn5 (Petty *et al.*, 2016). (B) *RTS1* overexpression promotes chromosome stability in *gcn5*Δ. Strains were transformed with a *URA3*-marked *SUP11* plasmid for colony color assay (Hieter *et al.*, 1985) along with vector control (–) and *RTS1* overexpressing (+) constructs, then plated at low density to grow without selection to observe rates of *SUP11* plasmid loss. From left to right, $n = 1756$, 1562, 1595, and 1953, with n representing the number of colonies scored. Shown are average rates of loss from three independent experiments; error bars indicate SD and stars indicate $p < 0.05$ by Student's unpaired t test (from left to right, $p = 0.003$ and 0.0007, respectively). (C) *RTS1* overexpression promotes timely cell division. Freshly transformed strains were arrested in G1, released, and analyzed by flow cytometry to monitor cell cycle progression. Shown are representative profiles 2 h after release from one of four independent experiments. (D) Rescue of nocodazole sensitivity by *RTS1* overexpression is shared among SAGA subunit mutants. Unique and shared mutants of the three Gcn5-containing complexes were transformed with indicated plasmid, grown to maintain selection, and plated with fivefold serial dilutions onto YPAD medium with or without 2 μg/ml nocodazole. Sensitivity and *RTS1* growth rescue were compared with *gcn5*Δ, and imaged after 3 d at 30°C. (E) Table of Gcn5 complex genes tested in D and the complex(es) in which they are found and corresponding molecular cartoons.

opposing spindle microtubules via kinetochores (Onn *et al.*, 2008). Of note, many of the genes encoding components of centromeres and kinetochores are essential and deeply conserved. For example, mistakes in orchestrating chromosome segregation can lead to aneuploidy, a common cause of birth defects in humans that is also detected in an overwhelming majority of solid tumors (Holland and Cleveland, 2012).

In many organisms, the centromere is defined by a histone H3 variant, CENP-A, along with centromere-specific DNA sequences (McKinley and Cheeseman, 2016). In budding yeast the centromere is defined by a single nucleosome containing the essential CENP-A H3 histone variant Cse4 (Stoler *et al.*, 1995; Meluh *et al.*, 1998; Furuyama and Biggins, 2007). Like canonical histones, Cse4 is dynamically modified, and many of the modifications that have been characterized thus far are notably involved in maintaining precise levels of Cse4 to prevent misincorporation at ectopic sites (Hewawasam *et al.*, 2010; Hildebrand and Biggins, 2016) or in directing Cse4 deposition (Samel *et al.*, 2012). There is a functional relationship between Gcn5 and Cse4 as well, evidenced by the extreme temperature sensitivity of the *gcn5*Δ *cse4-1* double mutant (Vernarecci *et al.*, 2008).

The kinetochore is a massive molecular structure that assembles onto the centromere and connects each sister chromatid to spindle microtubule(s) emanating from opposing poles. Sister chromatid cohesion is guarded by the spindle assembly checkpoint (SAC) until all kinetochores are properly attached to spindle microtubules. Dynamic phosphorylation is key for the checkpoint's execution, with multiple kinases and phosphatases acting in opposition to one another (Nasa and Kettenbach, 2018). For example, the Mps1 kinase monitors microtubule attachment by phosphorylating unattached kinetochore proteins to recruit SAC components, with the PP1 phosphatase acting to reverse Mps1 phosphorylation (Liu *et al.*, 2010; London *et al.*, 2012; Shepperd, Meadows, Sochaj, *et al.*, 2012; Yamagishi *et al.*, 2012; Primorac, Weir, Chiroli, *et al.*, 2013). An ongoing question is the extent to which novel interactions between enzymatic activities contribute to SAC silencing.

We previously characterized a genetic interaction between Gcn5 and the phosphoprotein phosphatase 2A (PP2A) regulatory subunit Rts1, such that overexpression of *RTS1* suppresses multiple *gcn5*Δ phenotypes, whereas loss of Rts1 is lethal in *gcn5*Δ cells (Petty *et al.*, 2016). There are two forms of PP2A in yeast that are distinguished by their regulatory subunits, Cdc55 or Rts1, which are homologous to mammalian B55 and B56 subunits, respectively (Figure 1A; Zhao *et al.*, 1997). Initial characterization of Rts1 revealed that its cellular localization depends on the cell cycle, and that it is recruited to centromeres during

metaphase of mitosis and meiosis by the Shugoshin protein Sgo1 (Gentry and Hallberg, 2002; Riedel, Katis, *et al.*, 2006; Yu and Koshland, 2007; Peplowska, Wallek, and Storchova, 2014). Together, Rts1 and Sgo1 contribute to sister chromatid cohesion protection in the tension-sensing checkpoint by blocking progression into anaphase if tensionless kinetochore–microtubule attachments are present (Riedel, Katis, *et al.*, 2006; Yu and Koshland, 2007; Nerusheva *et al.*, 2014; Peplowska, Wallek, and Storchova, 2014; Jin *et al.*, 2017).

We report here that *gcn5*Δ chromosome segregation defects are alleviated by increased dosage of *RTS1*. Further, loss of Gcn5 reduces the centromeric localization of Rts1 in metaphase-arrested cells. We identify three residues of Cse4 that affect *RTS1* dosage rescue of *gcn5*Δ phenotypes and specifically identify Cse4-S180 as a critical residue for localization of Rts1 to centromeres. These results broaden the evidence for a role for Gcn5 in the tension-sensing checkpoint and understanding of the deeply conserved Gcn5 acetyltransferase in the critical process of chromosome segregation.

RESULTS

RTS1 is a high-copy suppressor of *gcn5*Δ chromosome segregation phenotypes

We previously reported that *RTS1* suppresses *gcn5*Δ's histone gene expression and cell cycle entry defects (Petty *et al.*, 2016). To determine whether *RTS1* could also suppress *gcn5*Δ phenotypes related to chromosome segregation, we began by using the *SUP11*-based minichromosome assay (Hieter *et al.*, 1985) to determine rates of loss as a proxy for genome stability. Briefly, cells carrying the *SUP11* plasmid will suppress the pink colony phenotype of *ade2* mutants, leading to white colonies. A colony that is half-pink and half-white indicates that the plasmid was lost in one of the daughter cells arising from the first division after plating. As expected, we observed a significantly greater proportion of half-sectored colonies in *gcn5*Δ mutants (Figure 1B) indicative of reduced genome stability. Overexpression of *RTS1* significantly reduced *SUP11* loss in *gcn5*Δ cells and further reduced loss in wild type. These results suggest that *RTS1* positively regulates accurate chromosome segregation.

Defects in chromosome segregation can slow G2/M progression. Indeed, this is a classic *gcn5*Δ phenotype. To determine whether *RTS1* overexpression can suppress sluggish G2/M passage, we tracked cell cycle profiles of cells initially synchronized in G1 with α-factor pheromone, and collected at 20-minute intervals for flow cytometric analysis. By 2 h, wild-type cells with and without *RTS1* overexpression had resumed dividing, whereas the *gcn5*Δ vector control cells remained predominantly in G2/M (Figure 1C). In *gcn5*Δ cells overexpressing *RTS1*, the G1 population was increased at 2 h, indicating restored and timely progression through G2/M.

Increased *RTS1* suppresses loss of SAGA function in chromosome segregation

Mutations affecting chromosome segregation can increase sensitivity to microtubule-destabilizing drugs (Ouspenski *et al.*, 1999; Lampson and Kapoor, 2006). The SAC was first characterized by the identification of the *MAD* (mitotic arrest deficient) and *BUB* (budding uninhibited by benzimidazole) genes in genetic screens for mutants that fail to arrest growth in the presence of microtubule poisons (Hoyt *et al.*, 1991; Li and Murray, 1991). We previously reported that *RTS1* overexpression suppresses *gcn5*Δ sensitivity to the microtubule drug nocodazole (Petty *et al.*, 2016). To genetically dissect whether the chromosome segregation phenotypes of *gcn5*Δ mutants were tied to Gcn5 function in one of its complexes and, further, whether *RTS1* suppression of nocodazole sensitivity was complex specific, we transformed mutants of genes encoding a combination of distinct and structural complex subunits with *RTS1* or 2 μM vector controls. Transformants were challenged by exposure to nocodazole (Figure 1D). We observed nocodazole sensitivity in *gcn5*Δ, *ahc1*Δ, *spt8*Δ, *spt20*Δ, and *rtg2*Δ transformants, indicating that microtubule poison sensitivity is a phenotype common to impaired function of all Gcn5-containing complexes. However, *RTS1* suppression of nocodazole sensitivity was observed specifically in *gcn5*Δ, *spt8*Δ, and *spt20*Δ mutants, suggesting that *RTS1* overexpression suppresses loss of SAGA function in chromosome segregation (Figure 1E).

SAGA is a well-defined transcriptional coactivator complex with an acute role in stress-induced gene activation (Huisinga and Pugh, 2004). There is mounting evidence for broad SAGA involvement in activation of most genes that is buffered by increased mRNA stability (Baptista *et al.*, 2017). Therefore, we hypothesized that loss of Gcn5 function may impair chromosome segregation due to loss of expression of key genes and used reverse transcription-quantitative PCR (RT-qPCR) to determine steady-state expression levels of *RTS1*, *SGO1*, and *CSE4* (Supplemental Figure S1). There was no significant change in their steady-state expression in *gcn5*Δ cells suggesting that the chromosome segregation phenotype is not due to loss of expression of these central players. This result is consistent with previous genome-wide analysis that identified *RTS1*, *SGO1*, and *CSE4* as TFIID-dominated genes (Huisinga and Pugh, 2004).

Several studies have suggested a direct role for SAGA subunits at the centromere. The SAGA deubiquitinase subunit Ubp8 promotes Psh1-directed proteolysis of excess Cse4 (Canzonetta *et al.*, 2015). Gcn5 has been genetically identified as a regulator of a tension-sensing motif on histone H3 and found directly bound at centromeres by chromatin immunoprecipitation (ChIP; Luo, Deng, *et al.*, 2016).

To determine whether centromeric localization of SAGA subunits was broadly shared, we analyzed patterns of SAGA subunit binding at the centromere that were reported in recent studies of asynchronous cell populations (Supplemental Figure S2). FLAG-tagged Cse4 ChIP-seq binding (Hildebrand and Biggins, 2016) was used to demarcate the centromere. SAGA subunits Spt3, Spt7, and Spt8 along with deubiquitinase Ubp8 were recently mapped using ChEC-seq (Baptista *et al.*, 2017) and Sgf73 localization by ChIP-seq (Mason *et al.*, 2017). There is a notable pattern of localization of all of the SAGA subunits at centromeric regions of chromosome III and IV (Cen III and Cen IV). As the cells used in these published studies were not synchronized to metaphase, the lower signal we observe may be due to the smaller population at this point in the cell cycle. Nonetheless, these observations collectively point to a direct role for SAGA at or near the centromere.

Sgo1 is required for *RTS1* suppression of *gcn5*Δ nocodazole sensitivity

Rts1 subcellular location changes during the cell cycle, but relies predominantly on Sgo1 for localization to the centromere during metaphase (Gentry and Hallberg, 2002; Nerusheva *et al.*, 2014; Peplowska, Wallek, and Storchova, 2014). We considered the possibility that if *RTS1* suppression of *gcn5*Δ's chromosome segregation phenotypes occurred at the centromere, it should be dependent on Sgo1. To test this, we used the *sgo1-N51I* mutant allele that has been shown to specifically disrupt Sgo1's binding to Rts1 (Xu, Cetin, *et al.*, 2009; Peplowska, Wallek, and Storchova, 2014). Notably, Sgo1 plays several critical roles in chromosome segregation, therefore although *sgo1-N51I* impairs Rts1 recruitment, its chromosome segregation and growth phenotypes are less severe than those observed in *sgo1*Δ (Peplowska, Wallek, and Storchova, 2014). We constructed double mutants of *sgo1-N51I* with *gcn5*Δ

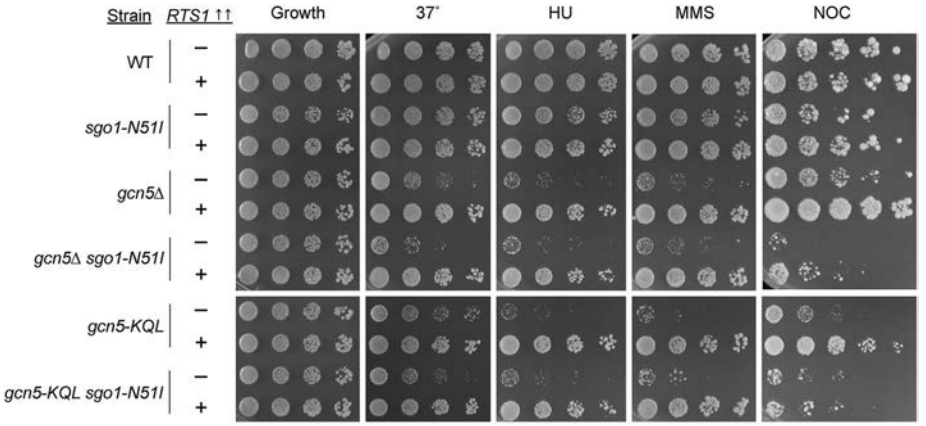

FIGURE 2: *RTS1* rescue of *gcn5*Δ nocodazole sensitivity requires Sgo1's Rts1-binding function. Overnight cultures of strains freshly transformed with vector control (–) or *RTS1* (+) were grown at 30°C and normalized. Fivefold serial dilutions were plated onto URA$^-$ plates and challenged with high temperature, 0.01% MMS, and 0.1 M HU. For nocodazole challenge (2 μg/ml), YPAD medium was used. The catalytic mutant *gcn5-KQL* (Wang, Liu, and Berger, 1998; Grant *et al.*, 1999) is also sensitive to nocodazole, and *RTS1* rescue of this phenotype requires Sgo1 binding. The increased nocodazole sensitivity in the *SGO1-TAP* background, relative to typical wild-type controls, suggests that the tag may partially interfere with Sgo1 function. Shown are representative images of four independent experiments.

and the catalytic mutant *gcn5-KQL* (Wang, Liu, and Berger, 1998), and then transformed the strains with *RTS1* or vector control plasmids to determine the effect of Sgo1 on *RTS1* suppression of *gcn5* phenotypes (Figure 2).

RTS1 overexpression suppressed *gcn5*Δ's temperature sensitivity as well as sensitivity to the DNA damaging agents hydroxyurea (HU) and methyl methanesulfanate (MMS), as we previously reported. We found that *sgo1-N51I* did not interfere with *RTS1* suppression of either *gcn5*Δ or *gcn5-KQL* sensitivity to heat nor DNA damage (Figure 2). However, the impact of *sgo1-N51I* on suppression of nocodazole sensitivity was markedly different. The *sgo-N51I* mutant exacerbated *gcn5*Δ and *gcn5-KQL* sensitivity to nocodazole and disrupted suppression by *RTS1*. Sensitivity was also exacerbated by *RTS1* overexpression in *SGO1-TAP* controls, similar to previous observations of overexpression improving *gcn5*Δ growth phenotypes while adversely affecting wild-type growth (Petty *et al.*, 2016). Overall, the fact that *RTS1* suppression of nocodazole sensitivity is abolished in *gcn5 sgo1-N51I* mutants points to Rts1 recruitment to the centromere by Sgo1 as key for the mechanism of suppression.

We considered the possibility that loss of *RTS1*-mediated suppression might be due to loss of Rts1 protein expression in *gcn5 sgo1-N51I* mutants. To address this, we integrated a single copy of Rts1 tagged with a triple PK epitope into the *RTS1* locus and constructed 2 μM–*RTS1*-3PK to evaluate Rts1 levels in log-phase wild-type, *sgo1-N51I*, *gcn5*Δ, and double-mutant populations. There were similar levels of single-copy Rts1 and Rts1 overexpression between all backgrounds, ruling out the possibility that loss of suppression was due to loss of expression (Supplemental Figure S3A). These results support the hypothesis that *RTS1* suppression of *gcn5*Δ chromosome segregation defects occurs at the centromere.

Gcn5 promotes Rts1 localization to the centromere

Sgo1 and Rts1 are recruited to the centromere and pericentromeric regions to prevent early release from the SAC in the presence of tensionless kinetochore microtubule attachments; they dissociate when sufficient tension is generated (Nerusheva *et al.*, 2014; Peplowska, Wallek, and Storchova, 2014; Jin *et al.*, 2017). Our data that *gcn5*Δ chromosome segregation phenotypes are rescued by *RTS1* overexpression in a manner dependent on Sgo1 recruitment led us to test whether there are changes in Rts1 localization to the centromere or pericentromere upon loss of Gcn5 and overexpression of Rts1. In addition to Rts1 centromeric localization, there are strong cytoplasmic and nuclear pools that interfered with attempts to address this question by quantitative microscopy, particularly in cells with *RTS1* overexpression. Therefore, we used the 3PK-tagged Rts1 integration and overexpression constructs to evaluate Rts1 centromere binding in wild type and *gcn5*Δ and *gcn5-KQL* under endogenous and overexpression conditions. We used nocodazole to arrest transformed cells in metaphase, confirmed by flow cytometry, and briefly fixed cells for ChIP. Rts1-3PK ChIP was followed by quantitative PCR (qPCR) using primers to amplify centromeric, pericentromeric, and distal loci on chromosome III as in Nerusheva *et al.* (2014). We observed lower Rts1 binding at both the centromere and pericentromere in *gcn5*Δ containing the vector control, but binding was restored to levels comparable to wild type with vector control upon *RTS1-3PK* overexpression (Figure 3A). The strongest signals were detected in the wild-type cells overexpressing *RTS1-3PK*. To determine whether this pattern was specific to Cen III, we also evaluated Rts1-3PK binding at the centromere, pericentromere, and a distal region of chromosome IV (Figure 3B). The results for Cen IV were very similar to those of Cen III, leading us to conclude that the pattern of lost Rts1 binding upon loss of Gcn5 is not specific to a single centromere. The Gcn5 catalytic mutant *gcn5-KQL* displayed similarly lower Rts1-3PK localization at both Cen III and Cen IV compared with wild type, indicating that it is loss of Gcn5's catalytic activity that interferes with Rts1 centromere localization in arrest conditions (Figure 3, A and B).

As with nocodazole sensitivity, it was possible that suppression of *gcn5*Δ's Rts1-binding defect would depend on Sgo1. We tested this by performing Rts1-3PK ChIP-qPCR in backgrounds with the *sgo1-N51I* mutation. Loss of Rts1-3PK was observed at the centromere and pericentromere of Chr IV in the *sgo1-N51I* single-mutant vector control and when combined with *gcn5*Δ (Figure 4). Unexpectedly, upon overexpression of *RTS1-3PK* in the *sgo1-N51I* mutant, increases in the ChIP signal were observed at the centromere and pericentromere, yet the strongest signal was at the nonspecific, distal arm locus. This result suggests that in the absence of Sgo1-specific recruitment, increased Rts1 may bind chromatin broadly and nonspecifically.

Directed Cse4 screen reveals roles for uncharacterized residues

Screens to evaluate the effects of mutations in individual histone residues are a powerful tool for uncovering new functional regions and potential sites of dynamic modification. Indeed, several sites of Cse4, H3, and H4 that contribute to chromosome segregation were originally identified in such screens (Camahort *et al.*, 2009; Luo *et al.*, 2010; Ng *et al.*, 2013). We hypothesized that the centromere-specific histone, Cse4, may be a target of Rts1 or Gcn5 activity and therefore screened alanine substitution mutants of serine, threonine, tyrosine,

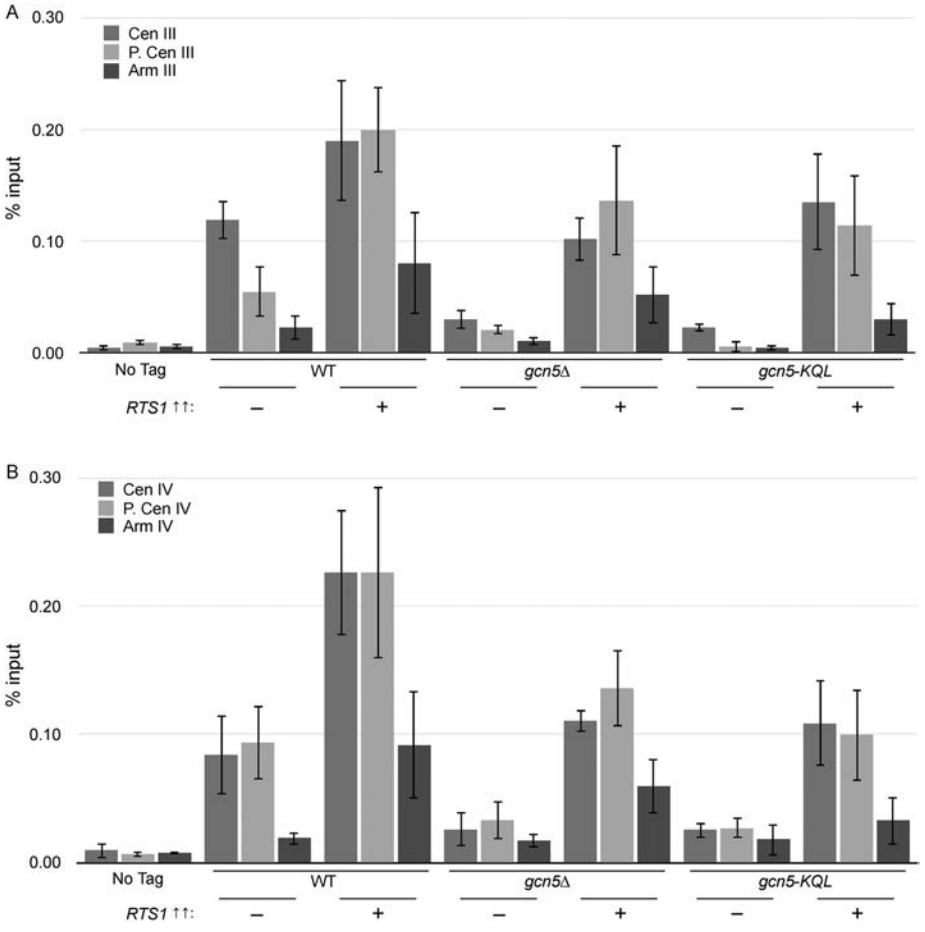

FIGURE 3: Gcn5 functions in *RTS1* localization to the centromere. Cells were arrested for 60–90 min with nocodazole (7.5 µg/ml) with arrest confirmed by light microscopy and flow cytometry. Metaphase-arrested transformants were fixed and analyzed for Rts1 binding at the centromere by chromatin immunoprecipitation using Rts1 tagged with the PK epitope (Nerusheva *et al.*, 2014; Verzijlbergen *et al.*, 2014) followed by qPCR amplification of centromeric (Cen), pericentromeric (P. Cen), and distal arm (Arm) of chromosomes III (A) and IV (B). Shown is the average of three independent experiments, with error bars indicating SD.

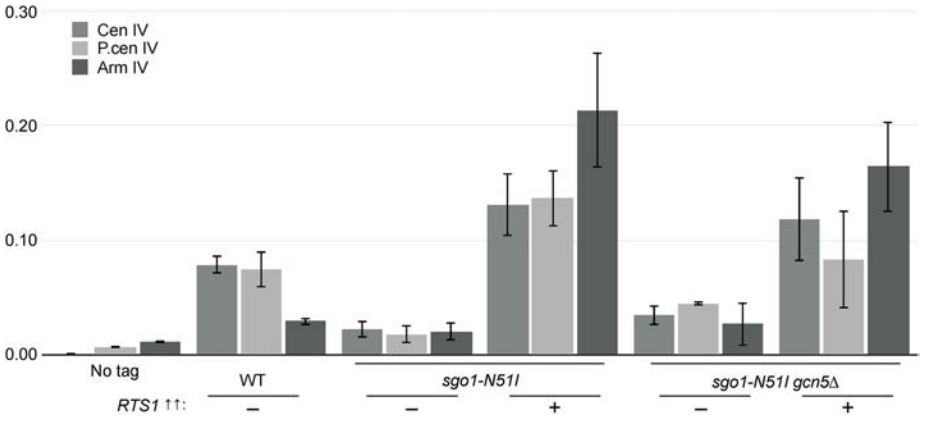

FIGURE 4: Binding specificity of overexpressed Rts1 is lost in *SGO1* mutants. Cells were grown, arrested with nocodazole (7.5 µg/ml), and fixed for Rts1-3PK ChIP as in Figure 3. In samples overexpressing *RTS1* with the *sgo1-N51I* mutation, the strongest Rts1-3PK ChIP signal is measured at the nonspecific Chr IV Arm locus, rather than at the centromere or pericentromere. Shown is the average of three independent experiments, with error bars indicating SD.

and lysine residues—possible sites for dynamic phosphorylation or acetylation—for effects on *gcn5*Δ phenotypes or rescue by *RTS1* overexpression (Figure 5A). For simplicity, we began the screen using a histone plasmid shuffle strategy, testing for effects of individual amino acid substitutions from the Cse4 alanine scanning mutagenesis library (Camahort *et al.*, 2009) on the temperature-sensitive phenotype of *gcn5*Δ. These initial results were somewhat complicated by the observation that plasmid-based expression of wild-type Cse4 itself caused mild temperature sensitivity, in addition to sensitivity to DNA damaging agents and nocodazole (unpublished data). Therefore, we selected candidates from the initial plasmid-based screen, generated HA-tagged versions of these mutations, and integrated them at the *CSE4* locus. The internal HA-tagged Cse4 construct was chosen based on published observations that it had minimal effects on Cse4 function in vivo, in contrast to other tags (Morey *et al.*, 2004). Upon integration, expression of each mutant was evaluated by anti-HA immunoblot (Supplemental Figure S3B). The mutations were tested for effects on a panel of *gcn5*Δ phenotypes and suppression by *RTS1* (Figure 5B). We found that wild-type HA-tagged Cse4 did not cause notable changes in growth in wild-type cells under any of the challenge conditions. This was in contrast to *gcn5*Δ cells, which did exhibit DNA damage sensitivity as expected. The *cse4-S135A* mutation further exacerbated *gcn5*Δ DNA damage sensitivity and interfered with *RTS1* suppression of these growth phenotypes, as did *cse4-S180A*. This mutant residue also interfered with *RTS1* suppression of temperature sensitivity.

The *cse4-K215A* mutation broadly exacerbated *gcn5*Δ growth defects in all conditions tested and even resulted in temperature and MMS sensitivity in otherwise wild-type cells (Supplemental Figure S4A). We hypothesized that this might be due to the loss of charge resulting from the alanine substitution. To test this, *cse4-K215R* strains were constructed and evaluated at elevated temperature and in the presence of nocodazole (Supplemental Figure S4B). Both growth and *RTS1* suppression of *gcn5*Δ temperature sensitivity were comparable in *CSE4* and *cse4-K215R* transformants. For nocodazole sensitivity, the *K215R* substitution appeared to improve *gcn5*Δ growth independently of *RTS1*. However, we also noted that unlike *cse4-K215A*, the *K215R* mutation caused temperature and nocodazole sensitivity in wild-type cells, and that *RTS1* overexpression

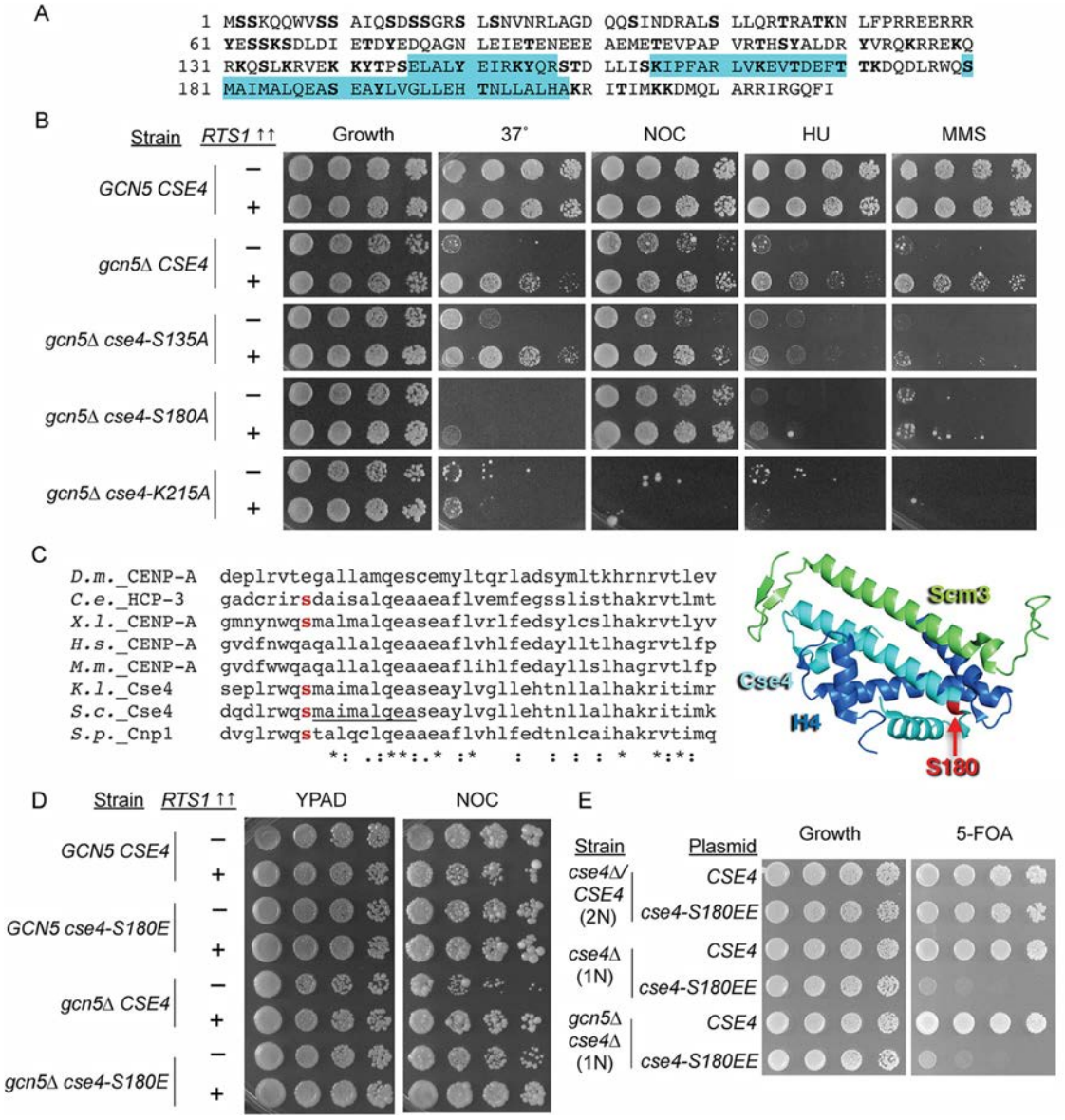

FIGURE 5: Directed screen identifies specific Cse4 residues that affect *gcn5*Δ rescue by *RTS1*. (A) Nonessential S, T, Y, and K residues of Cse4 (57; bold) were individually screened for function in rescue by increased *RTS1* dosage for a battery of *gcn5*Δ sensitivities. The alpha helices of the histone fold domain are highlighted in blue. (B) Candidate *cse4* substitution mutations of interest were integrated into the genome to confirm results of an initial plasmid shuffle screen. Cultures of freshly transformed strains were normalized, plated onto URA$^-$ plates, and challenged to grow at high temperature (37°C), and in the presence of DNA damaging agents HU (0.05 M) and MMS (0.015%). For nocodazole (2 μg/ml), YPAD medium was used. (C) Cse4-S180 is within the conserved C-terminal region of Cse4. Clustal W (Thompson *et al.*, 1994) was used to generate an alignment of CENP-A homologues. Cse4-S180 and the corresponding conserved S residues in *X. laevis*, *C. elegans*, *K. lactis*, and *S. pombe* are shown in red bold font, and the Scm3-binding motif (Zhou, Feng, *et al.*, 2011) is underlined. The NMR structure of *K. lactis* Cse4 (cyan), Scm3 (green), and H4 (blue) is shown with S180 corresponding residue highlighted in red (Cho and Harrison, 2011). (D) Integrated *cse4-S180E* substitution rescues nocodazole sensitivity similarly to *cse4-180A*. Growth of fresh transformants was challenged as above and assessed after 3 d. (E) Recapitulating phosphorylation charge change by *cse4-S180EE* mutation is lethal. Plasmid shuffle by plating onto media containing 5-FOA was used to select for cells having lost the *CSE4-URA3* covering plasmid. Representative images of at least four independent experiments are shown.

restored growth at high temperature. By comparison, the acetyl-mimetic *cse4-K215Q* mutant (Supplemental Figure S4C) reversed the phenotypes in the wild-type background and improved growth at high temperature in the *gcn5*Δ background. These results suggest that the charge and potential acetylation of Cse4-K215 contribute to a temperature-sensitive function of Cse4. Although found within the conserved histone fold region of CENP-A/Cse4, K215 is not conserved in the major model organisms that we surveyed, so this function may be unique to *Saccharomyces cerevisiae*.

We were particularly interested in effects of the *cse4-S180A* mutation due to the conservation of this residue among yeast species and some metazoans, and its proximity to the recognition motif for binding by Scm3, the chaperone that integrates Cse4 into chromatin (Figure 5C; S180 is shown in red and Scm3 recognition motif

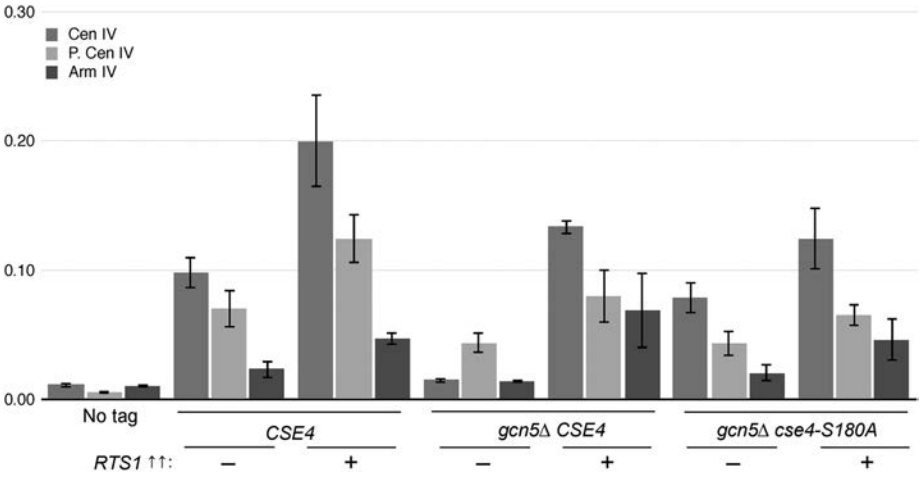

FIGURE 6: The *cse4-S180A* mutant restores Rts1 binding at centromere IV in metaphase-arrested cells. Integrated *cse4-S180A* mutant strains were transformed with vector (–) or *RTS1* (+) 2 μM plasmids and grown, arrested in metaphase, and fixed for ChIP as described. For *gcn5*Δ *cse4-S180A*, a nocodazole concentration of 2 μg/ml was used to enrich for metaphase cells; for all other strains 7.5 μg/ml was used. Rts1 binding at centromeric, pericentromeric, and distal arm loci was assessed by qPCR. Shown are average percent input values of three independent experiments; error bars indicate SD.

underlined). We found that *cse4-S180A* alleviated *gcn5*Δ nocodazole sensitivity, and that growth was further improved by *RTS1* overexpression (Figure 5B). There was also a reduction in the number of suppressor colonies among *gcn5*Δ *cse4-S180A* growth when challenged by nocodazole. We hypothesized that S180 could be a site of critically dynamic phosphorylation and generated a *cse4-S180E* phosphomimetic mutant to test this possibility genetically. The effect of *cse4-S180E* on *gcn5*Δ nocodazole sensitivity was similar to *cse4-S180A* (Figure 5D); therefore, disruption of this site may be sufficient to improve a function related to microtubule stress. Alternatively, although glutamate is commonly used to genetically mimic constitutive phosphorylation, a single glutamate substitution does not faithfully recapitulate the charge change of serine phosphorylation. Previous work has demonstrated that single serine to glutamate substitutions can have the same phenotype as alanine substitution, whereas replacement of serine with two glutamates, yielding a charge change analogous to phosphorylation, resulted in phenotypes more similar to constitutive phosphorylation (Strickfaden *et al.*, 2007). Therefore, we generated a second *cse4* phosphomimetic mutant substituting two glutamate residues for S180. Multiple failed integration attempts in haploids led us to test the viability of the *cse4-S180EE* mutation using a plasmid shuffle strategy. We transformed a *cse4*Δ/*CSE4* diploid and *cse4*Δ and *gcn5*Δ *cse4*Δ haploids containing a *URA3*-marked *CSE4* plasmid with either a *TRP1*-marked *HA-CSE4* or *HA-cse4-S180EE* plasmid. The transformants were then challenged to grow on medium containing 5-fluoroorotic acid (5-FOA) to select for cells that could lose the *URA3* covering plasmid (Figure 5E). Haploids selected for the *cse4-S180EE* plasmid as the sole source of Cse4 were inviable. We confirmed expression of HA-*cse4-S180EE* in diploid transformants by immunoblot, ruling out loss of expression as the cause of inviability (Supplemental Figure S6). Rather, these data reveal toxicity of a constitutive charge change mimicking S180 phosphorylation.

Cse4-S180 contributes to centromeric localization of Rts1

The observation that *cse4-S180A* suppressed *gcn5*Δ nocodazole sensitivity raised the possibility that this might be due to restored localization of Rts1 to the centromere in metaphase cells. This idea was tested by ChIP of Rts1-3PK in the HA-tagged Cse4 and *cse4-S180A* strains in wild-type and *gcn5*Δ backgrounds, with and without *RTS1* overexpression. During optimization of metaphase arrest conditions, we noted that the high concentration of nocodazole used for arrest is toxic to *gcn5*Δ *cse4-S180A*, so a reduced concentration of 2 μg/ml was used to delay the cell cycle and enrich for metaphase cells as shown in Wang and Burke (1995). Interestingly, this lower nocodazole concentration does not completely disrupt kinetochore microtubules (Wang and Burke, 1995), suggesting that although the *cse4-S180A* mutation alleviated *gcn5*Δ sensitivity to a cell cycle delay by nocodazole, some microtubule structure is required for viability. We again evaluated Rts1 binding at and around Cen IV using qPCR in wild-type (Supplemental Figure S5) and *gcn5*Δ backgrounds (Figure 6). Compared to wild type, *cse4-S180A* slightly reduced Rts1 levels at the centromere and pericentromere in cells containing Gcn5, but in *gcn5*Δ, there was increased Rts1 at the centromere. Overexpression of *RTS1* led to further increases of Rts1 at the centromere in *GCN5* cells, although not to the extent as when Cse4 is wild type, and further increases at both the centromere and pericentromere in *gcn5*Δ cells. To determine whether these differences in Rts1 binding were due to altered Rts1-3PK expression/overexpression, we used quantitative immunoblotting of lysates prepared in parallel with samples prepared for ChIP. We observed consistent levels of Rts1-3PK in cells carrying a single copy and cells containing the 2 μm–*RTS1-3PK* high-copy plasmid from strain to strain (Supplemental Figure S6, A and B). At the same time, we observed levels of Cse4 expression and noted a reduction in *cse4-S180A* in both Gcn5-containing and deletion backgrounds. These results point to a role for Cse4-S180 in promoting Rts1 localization to centromeres in the absence of Gcn5 and reveal a potential role in regulation of Cse4 levels independent of transcription.

DISCUSSION

Our data reveal opposing roles for Gcn5 and Cse4-S180 in the localization of Rts1 in the mitotic spindle tension-sensing pathway (Figure 7). Loss of function of any Gcn5-containing complex results in sensitivity to microtubule stress but it is specifically the loss of SAGA that can be suppressed by *RTS1* overexpression. *RTS1*-mediated suppression of *gcn5*Δ nocodazole sensitivity requires recruitment of Rts1 to the centromere by Sgo1. We characterized a new role for Gcn5 acetyltransferase activity in promoting Rts1 localization to low-tension centromeres. Finally, we identified Cse4-S180 as a negative regulator of Rts1 localization to centromeres in *gcn5*Δ cells and demonstrated that the phosphomimetic *cse4-S180EE* mutation is lethal, indicating a potentially critical role for tightly regulated phosphorylation at this site.

Previous genetic screens have identified functions for H3 and H4 residues in chromosome segregation (Luo *et al.*, 2010; Ng *et al.*, 2013). Indeed, three residues of H3 (K42, G44, and T45) function in centromeric tension sensing and growth phenotypes caused by mutations to these residues can be suppressed by loss of Gcn5 acetyltransferase activity (Luo, Deng, *et al.*, 2016). This suggests that under normal conditions, Gcn5 positively regulates

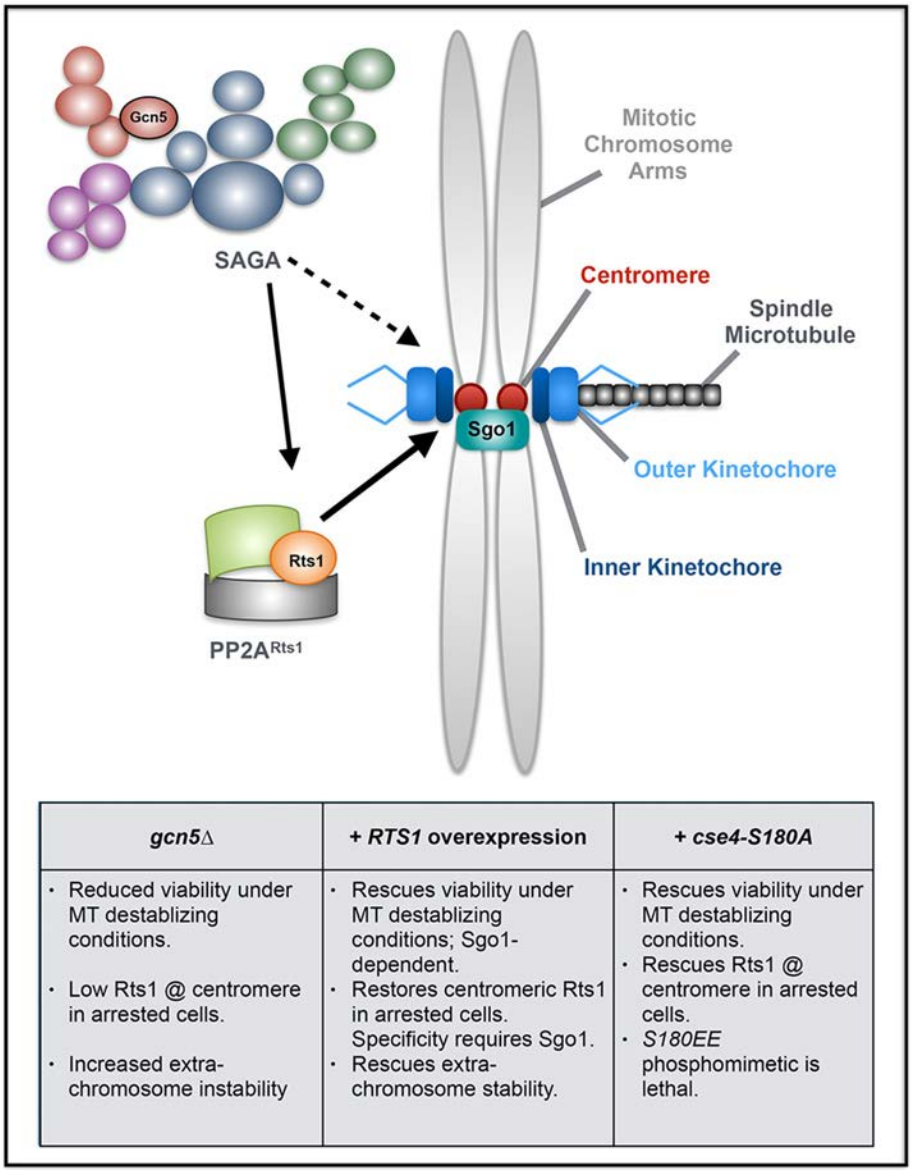

*gcn5*Δ	+ *RTS1* overexpression	+ *cse4-S180A*
• Reduced viability under MT destablizing conditions. • Low Rts1 @ centromere in arrested cells. • Increased extra-chromosome instability	• Rescues viability under MT destablizing conditions; Sgo1-dependent. • Restores centromeric Rts1 in arrested cells. Specificity requires Sgo1. • Rescues extra-chromosome stability.	• Rescues viability under MT destablizing conditions. • Rescues Rts1 @ centromere in arrested cells. • *S180EE* phosphomimetic is lethal.

FIGURE 7: Gcn5 promotes Rts1 localization to centromeres. The tension-sensing checkpoint ensures that sister chromatids do not separate before opposing spindle microtubules are properly attached. We propose that under low-tension conditions, depicted here as only one chromatid attached to a microtubule (MT), Gcn5 acts within SAGA to promote Rts1 localization to the centromere. In the absence of Gcn5 or in a catalytic mutant, overexpression of *RTS1* can restore its centromeric localization, but localization specificity requires Sgo1. The centromere (shown in red) is defined by the presence of a histone H3 variant Cse4-containing nucleosome. We report a role for the conserved Cse4-S180 residue in promoting Rts1 centromeric localization in the absence of Gcn5. For simplicity, the condensin, cohesin, and chromosome passenger complexes, also active in centromeric checkpoints, are not shown, but among their subunits are potential targets of Gcn5 and PP2A-Rts1 activities.

tension sensing during mitosis. The nocodazole sensitivity of multiple Gcn5-complex subunit mutants that we observed is consistent with chromosome transmission fidelity phenotypes of *sgf11*Δ and *sgf73*Δ and of *spt8*Δ's abnormal chromosome maintenance phenotype reported previously in large-scale studies (Theis *et al.*, 2010; Stirling *et al.*, 2011). Because *RTS1* overexpression suppressed nocodazole sensitivity in the SAGA mutants tested herein, we conclude that *RTS1* suppresses loss of SAGA function in chromosome segregation. We also determined localization of Sgf73, Ubp8, Spt8, and Spt7 at or around centromeres by mining high-resolution data sets. We propose that it is Gcn5's function in SAGA at the centromere that promotes mitotic tension sensing (Figure 7).

Our finding that Gcn5 acetyltransferase activity is required for Rts1 localization to centromeres indicates that there may be new centromere and/or kinetochore targets of Gcn5 acetylation. Indeed, Cse4-K49 has been identified as acetylated by mass spectrometry (Boeckmann, Takahashi, Au, *et al.*, 2013) and is likely a Gcn5 substrate (Popsel, 2015). Our identification of growth phenotypes in the *cse4-K215A/R* mutants that were reversed by *cse4-K215Q* acetylmimetic mutation raises the possibility that this C-terminal residue is another site of Gcn5 acetylation. The chromosome passenger complex (CPC) subunits Bir1 and Sli15 have been identified as potential Gcn5 substrates (Downey *et al.*, 2015) and potential PP2A-Rts1 (Zapata *et al.*, 2014) substrates by quantitative phosphoproteomics. The CPC is required for activation, maintenance, and silencing of the SAC (Carmena, Wheelock, *et al.*, 2012), suggesting that both Gcn5 acetylation and PP2A contribute to CPC function.

Suppression of *gcn5*Δ nocodazole sensitivity by *RTS1* overexpression requires Sgo1's binding function for Rts1 (Figure 4). On the basis of this result, we fully expected to observe loss of Rts1 centromere binding in strains with the *sgo1-N51I* mutation. Instead, there was increased centromeric localization of overexpressed Rts1-3PK, and elevated binding at all sites tested. Indeed, this is akin to observations that overexpressed CENP-A/Cse4 can misincorporate into noncentromeric chromatin and bypass the requirement for its chaperone Scm3 (Camahort *et al.*, 2009; Hildebrand and Biggins, 2016), raising a possibility for parallel Cse4-Rts1 mislocalization.

We also found that the Cse4 histone variant itself functions in regulating Rts1 binding to centromere, in that *cse4-S180A* partially increases Rts1's centromeric localization in *gcn5*Δ cells. It has been recently reported that Cse4 directly interacts with the N-terminal region of Sgo1, and this interaction is sufficient to recruit Sgo1 to the centromere (Mishra *et al.*, 2017). It is not known what region of Cse4 Sgo1 recognizes, therefore a straightforward possibility is that Cse4-S180 functions in the Sgo1-Cse4 physical interaction. Alternatively, the fact that Cse4-S180 is directly adjacent to the Scm3-binding motif of Cse4 (Zhou, Feng, *et al.*, 2011) suggests that mutating this residue may also alter dynamics between Cse4 and its chaperone.

Phosphorylated serine residues at the N-terminus of Cse4 were previously found to be conserved sites of modification (Boeckmann, Takahashi, Au, *et al.*, 2013), so the fact that Cse4-S180 is

conserved in *Kluyveromyces lactis* and *Schizosaccharomyces pombe* as well as metazoans *Caenorhabditis elegans* and *Xenopus laevis* lends credence to the possibility that S180 is a site of functional significance and potential dynamic phosphorylation. Further, S180 is conserved in human H3 variants, which may reflect functions beyond chromosome segregation. A need for controlled, dynamic regulation of phosphorylation at this site is supported by the lethality caused by the *cse4-S180EE* mutation. Our observation that *cse4-S180*A alleviates *gcn5*Δ sensitivity to chronic, low-level microtubule destabilization by nocodazole, but exacerbates sensitivity to acute treatment, clearly points to the mechanism of suppression involving microtubules. Previously, N-terminal Cse4 phosphomimetic mutants were found to suppress mutations to the kinase Ipl1, a subunit of the CPC, and Ipl1 kinetochore targets, but to exacerbate growth and chromosome segregation phenotypes of kinetochore assembly mutants. These observations support a role for Cse4 N-terminal phosphorylation by Ipl1 in destabilizing kinetochore–microtubule attachments (Boeckmann, Takahashi, Au, *et al.*, 2013). If a similar mechanism is at play with Cse4-S180, the nonphosphorylatable *cse4-S180A* mutant may stabilize kinetochore–microtubule attachments, whereas persistent phosphorylation may prevent stable attachments from forming, leading to lethality.

The new connections we report between Cse4 residues (S135, S180) and Rts1, and Cse4 expression are also of note considering its regulation. Ordinarily, Cse4 is tightly regulated by lysine ubiquitin-mediated proteolysis by multiple E3 ligases, most notably by Psh1 and the SUMO-targeted ubiquitin ligase, Slx5 (Hewawasam *et al.*, 2010; Ranjitkar *et al.*, 2010; Au *et al.*, 2013; Ohkuni *et al.*, 2016, 2018). Psh1 recognizes Cse4's CENP-A targeting domain and S180 is within that key region (Ranjitkar *et al.*, 2010), and Scm3 chaperone binding at the centromere is thought to protect from Psh1-mediated degradation (Hewawasam *et al.*, 2010). Therefore, if *cse4-S180A* impairs Scm3 binding, it may be more prone to degradation, which is in line with our observation that HA-Cse4-S180A levels are lower than wild type. Moreover, constitutively stable Cse4 is toxic to yeast cells and stable or overexpressed Cse4 mislocalizes to euchromatin (Collins *et al.*, 2004; Hildebrand and Biggins, 2016). Similarly, increased expression of CENP-A is a prognostic biomarker of human cancers and overexpression causes chromosomal instability in human cell lines (Sun *et al.*, 2016; Shrestha *et al.*, 2017). Alterations in levels observed in the *cse4-S135A* mutant may be due to increased Cse4 stability by altering proteolysis dynamics. Further phenotypic analysis of phosphomimetic mutants may yet reveal proteolytic-independent functions.

Much has been learned about the structural components and regulatory partners that ensure faithful chromosome segregation, from centromere-specific histone variant Cse4, to the dozens of subunits comprising the kinetochore, to the multiple kinase–phosphatase partners that function in the SAC. Ultimately, it seems reasonable to expect that Gcn5 and PP2A-Rts1 targeting of centromeric chromatin, including CENP-A/Cse4, and kinetochore/SAC substrates, contribute to mitotic SAC silencing through the critical tension-sensing checkpoint. The human SAGA complex is an activator of the oncoprotein c-MYC and Gcn5 acetylates regulatory regions of c-MYC targets for activation, driving cancerous transformation (Liu *et al.*, 2003; Patel *et al.*, 2004; Wang and Dent, 2014). The functional conservation of kinetochore components and regulatory mechanisms suggests that the work reported here may also lead to an expanded understanding of the role for SAGA in the mechanisms underlying aneuploidy that is so commonly found in human cancers.

MATERIALS AND METHODS

Yeast growth, strains, and plasmids

Yeast strains used in this work are in the W303 background as listed in Supplemental Table S1. Cells were grown in synthetic dropout or yeast extract–peptone–adenine–dextrose (YPAD) liquid medium under standard growth conditions (Guthrie and Fink, 1991) at 30°C except where indicated. For plate assays, cells from overnight cultures were normalized to A_{600} of 1 and 1:5 serial dilutions were pinned onto plates to grow for 3 d in the presence of an indicated challenge. Plates were photographed after 3 d growth. Drug concentrations are listed in corresponding figure legends. Plasmids used are listed in Supplemental Table S2. Independent lithium acetate transformations were used for biological replicates of all experiments (Amberg *et al.*, 2005). For the minichromosome loss assay, transformants were grown under URA-LEU selection, then diluted in LEU^- synthetic medium for two doublings (4–6 h of growth) before plating onto LEU^- plates at a concentration of 500 cells per plate. Colony color and sectoring was assayed as described (Hieter *et al.*, 1985). The Cse4 mutant screen was performed by plasmid shuffle using plasmids from the Cse4 plasmid library (Camahort *et al.*, 2009). Site-directed mutagenesis of the pRB294 *(HA)3-(HIS)6-CSE4* construct (Baker and Rogers, 2006) was used to generate tagged Cse4 mutants for insertion into the *CSE4* locus (Amberg *et al.*, 2005). Cse4 integrants were screened by molecular genotyping and backcrossed once to wild type. Newly constructed strains generated through crosses were sporulated using minimal sporulation media (Rose *et al.*, 1990) before dissection and genotyping.

α-Factor arrest and flow cytometry

Isogenic *bar1*Δ strains were used for α-factor sensitization. Growth, arrest, and recovery were performed at 30°C. Overnight cultures of transformants were grown in URA and diluted to 0.1 A_{600} in YPAD the next morning. At 0.3 A_{600}, α-factor was added to the cultures for 90–120 min and arrest was monitored by light microscopy. To release, cells were collected, washed twice in prewarmed YPAD, and the T_0 sample was collected before resuming growth at 30°C. Samples were collected every 15 min for 4 h and fixed in 70% ethanol overnight at 4°C. Fixed cells were processed and stained with propidium iodide before analyzing for DNA content with a BD Accuri C6 Flow Cytometer as in Petty *et al.* (2016).

Rts1-3PK ChIP

Transformants were grown overnight in URA^- or LEU^- medium, diluted into 10 ml URA^- or LEU^- cultures to grow to 1.0 A_{600}. Cultures were then diluted to 0.1 A_{600} in 50 ml YPAD and grown to 0.2–0.3 A_{600} before addition of nocodazole (Sigma M1404) at 7.5 µg/ml for most strains; 2 µg/ml was used for *gcn5*Δ *cse4-S180A RTS1-3PK::TRP1* (LPY22275) and arrested for 90–120 min. Arrest was monitored by light microscopy and subsequently confirmed by flow cytometry using samples removed at onset of treatment and just before fixation. Metaphase-arrested cells were fixed for 15 min at room temperature by addition of 1.2 ml 37% formaldehyde. Cells were lysed and sonicated for ChIP as described (Torres-Machorro *et al.*, 2015) and 400 µg of sample was used per IP with anti-V5 (MCA1360; Bio-Rad), which recognizes the PK epitope. ChIP DNA was recovered using the Qiagen PCR purification kit. qPCR was completed using an Opticon Monitor 2 and Eurogentec qPCR MasterMix Plus. Primer pairs *CEN4 150bp R, CEN4.2, CEN3 250bp R, CEN3 2.6kb R,* and *ChIII 103kb R* from Nerusheva *et al.* (2014) along with a newly designed *ArmIV 112kb R* (Supplemental Table S3) were used to amplify centromeric, pericentromeric, and distal targets for ChIP and input DNA. ChIP signals were quantified relative to input.

RT-qPCR

Wild-type and *gcn5*Δ cells were grown in 20 ml cultures to log phase at 30°C before RNA extraction by the hot phenol method. Samples were treated with DNase (Ambion) and cDNA prepared with the TaqMan Reverse Transcriptase kit (Life Sciences). Primers for *ADH1*, *CWP1*, and *SCR1* controls are as listed in Petty *et al.* (2016); *GCN5*, *RTS1*, and *SGO1* primers are listed in Supplemental Table S3. Otherwise, qPCR was completed as above, normalized to RNA polymerase III transcript *SCR1*, an established *GCN5*-independent control, and *gcn5*Δ expression relative to wild type was determined.

Protein lysate preparation and immunoblotting

Overnight cultures of transformants were grown in selective media and diluted to 0.15 A_{600} the following morning. Cells were collected at 0.8 A_{600} and lysates were prepared as described (Clarke *et al.*, 1999). Acrylamide gels (12%) were used for SDS–PAGE separation of HA-Cse4, Rts1-3PK, and tubulin, which were then detected by immunoblotting on nitrocellulose (0.2 μM; Prometheus). Anti-V5 was used at 1:10,000, anti-HA 1:2000, and anti-tubulin 1:20,000 in 3% milk in Tris-buffered saline-Tween. Anti-mouse and rabbit immunoglobulin G horseradish peroxidase–conjugated secondary antibodies (Promega) were used at 1:20,000. Blots were exposed to Pierce ECL Western Blot Substrate (Thermo Fisher) and images collected using a Protein Simple FluorChem E imager. Relative quantification was determined by signal density analysis in ImageJ (Schneider *et al.*, 2012).

ACKNOWLEDGMENTS

We thank R. Baker, S. Biggins, J. Gerton, P. Hieter, A. Marston, F. Spencer, and Z. Storchova for generously sharing strains, plasmids, and advice. We also thank current and past lab members for critical feedback throughout the project and during preparation of the manuscript. American Cancer Society Postdoctoral Fellowship PF-13-283-01 and a Frontiers in Innovation Scholars Program award from the University of California, San Diego (UCSD), supported E.P. Support for M.E. was provided by the Cell and Molecular Genetics Training Program: 5T32GM007240. This work was initiated with support from National Institutes of Health (NIH) GM090177. Additional support for the project was from National Science Foundation Grant no. MCB-1716841, NIH Grant no. AG-056440, the University of California Cancer Research Coordinating Committee, and the UCSD Academic Senate.

REFERENCES

Boldface names denote co–first authors.

Amberg D, Burke D, Strathern SJ (2005). Methods in Yeast Genetics: A Cold Spring Harbor Laboratory Course Manual, Cold Spring Harbor, NY: Cold Spring Harbor Laboratory Press.

Au WC, Dawson AR, Rawson DW, Taylor SB, Baker RE, Basrai MA (2013). A novel role of the N terminus of budding yeast histone H3 variant Cse4 in ubiquitin-mediated proteolysis. Genetics 194, 513–518.

Baker RE, Rogers K (2006). Phylogenetic analysis of fungal centromere H3 proteins. Genetics 174, 1481–1492.

Baptista T, Grunberg S, Minoungou N, Koster MJE, Timmers HTM, Hahn S, Devys D, Tora L (2017). SAGA is a general cofactor for RNA polymerase II transcription. Mol Cell 68, 130–143, e135.

Boeckmann L, Takahashi Y, Au WC, Mishra PK, Choy JS, Dawson AR, Szeto MY, Waybright TJ, Heger C, McAndrew C, *et al.* (2013). Phosphorylation of centromeric histone H3 variant regulates chromosome segregation in *Saccharomyces cerevisiae*. Mol Biol Cell 24, 2034–2044.

Camahort R, Shivaraju M, Mattingly M, Li B, Nakanishi S, Zhu D, Shilatifard A, Workman JL, Gerton JL (2009). Cse4 is part of an octameric nucleosome in budding yeast. Mol Cell 35, 794–805.

Canzonetta C, Vernarecci S, Iuliani M, Marracino C, Belloni C, Ballario P, Filetici P (2015). SAGA DUB-Ubp8 deubiquitylates centromeric histone variant Cse4. G3 (Bethesda) 6, 287–298.

Carmena M, Wheelock M, Funabiki H, Earnshaw WC (2012). The chromosomal passenger complex (CPC): from easy rider to the godfather of mitosis. Nat Rev Mol Cell Biol 13, 789–803.

Cho US, Harrison SC (2011). Recognition of the centromere-specific histone Cse4 by the chaperone Scm3. Proc Natl Acad Sci USA 108, 9367–9371.

Clarke AS, Lowell JE, Jacobson SJ, Pillus L (1999). Esa1p is an essential histone acetyltransferase required for cell cycle progression. Mol Cell Biol 19, 2515–2526.

Collins KA, Furuyama S, Biggins S (2004). Proteolysis contributes to the exclusive centromere localization of the yeast Cse4/CENP-A histone H3 variant. Curr Biol 14, 1968–1972.

Downey M, Johnson JR, Davey NE, Newton BW, Johnson TL, Galaang S, Seller CA, Krogan N, Toczyski DP (2015). Acetylome profiling reveals overlap in the regulation of diverse processes by sirtuins, Gcn5, and Esa1. Mol Cell Proteomics 14, 162–176.

Eberharter A, Sterner DE, Schieltz D, Hassan A, Yates JR, Berger SL 3rd, Workman JL (1999). The ADA complex is a distinct histone acetyltransferase complex in *Saccharomyces cerevisiae*. Mol Cell Biol 19, 6621–6631.

Furuyama S, Biggins S (2007). Centromere identity is specified by a single centromeric nucleosome in budding yeast. Proc Natl Acad Sci USA 104, 14706–14711.

Gentry MS, Hallberg RL (2002). Localization of *Saccharomyces cerevisiae* protein phosphatase 2A subunits throughout mitotic cell cycle. Mol Biol Cell 13, 3477–3492.

Grant PA, Duggan L, Cote J, Roberts SM, Brownell JE, Candau R, Ohba R, Owen-Hughes T, Allis CD, Winston F, *et al.* (1997). Yeast Gcn5 functions in two multisubunit complexes to acetylate nucleosomal histones: characterization of an Ada complex and the SAGA (Spt/Ada) complex. Genes Dev 11, 1640–1650.

Grant PA, Eberharter A, John S, Cook RG, Turner BM, Workman JL (1999). Expanded lysine acetylation specificity of Gcn5 in native complexes. J Biol Chem 274, 5895–5900.

Guthrie C, Fink GR (1991). Guide to Yeast Genetics and Molecular Biology, San Diego: Academic Press.

Hewawasam G, Shivaraju M, Mattingly M, Venkatesh S, Martin-Brown S, Florens L, Workman JL, Gerton JL (2010). Psh1 is an E3 ubiquitin ligase that targets the centromeric histone variant Cse4. Mol Cell 40, 444–454.

Hieter P, Mann C, Snyder M, Davis RW (1985). Mitotic stability of yeast chromosomes: a colony color assay that measures nondisjunction and chromosome loss. Cell 40, 381–392.

Hildebrand EM, Biggins S (2016). Regulation of budding yeast CENP-A levels prevents misincorporation at promoter nucleosomes and transcriptional defects. PLoS Genet 12, e1005930.

Holland AJ, Cleveland DW (2012). Losing balance: the origin and impact of aneuploidy in cancer. EMBO Rep 13, 501–514.

Howe L, Auston D, Grant P, John S, Cook RG, Workman JL, Pillus L (2001). Histone H3 specific acetyltransferases are essential for cell cycle progression. Genes Dev 15, 3144–3154.

Hoyt MA, Totis L, Roberts BT (1991). *S. cerevisiae* genes required for cell cycle arrest in response to loss of microtubule function. Cell 66, 507–517.

Huisinga KL, Pugh BF (2004). A genome-wide housekeeping role for TFIID and a highly regulated stress-related role for SAGA in *Saccharomyces cerevisiae*. Mol Cell 13, 573–585.

Jin F, Bokros M, Wang Y (2017). Premature silencing of the spindle assembly checkpoint is pPrevented by the Bub1-H2A-Sgo1-PP2A axis in *Saccharomyces cerevisiae*. Genetics 205, 1169–1178.

Kornberg RD, Lorch Y (1999). Twenty-five years of the nucleosome, fundamental particle of the eukaryote chromosome. Cell 98, 285–294.

Lampson MA, Kapoor TM (2006). Unraveling cell division mechanisms with small-molecule inhibitors. Nat Chem Biol 2, 19–27.

Lee KK, Sardiu ME, Swanson SK, Gilmore JM, Torok M, Grant PA, Florens L, Workman JL, Washburn MP (2011). Combinatorial depletion analysis to assemble the network architecture of the SAGA and ADA chromatin remodeling complexes. Mol Syst Biol 7, 503.

Li R, Murray AW (1991). Feedback control of mitosis in budding yeast. Cell 66, 519–531.

Liu X, Tesfai J, Evrard YA, Dent SY, Martinez E (2003). c-Myc transformation domain recruits the human STAGA complex and requires TRRAP and

GCN5 acetylase activity for transcription activation. J Biol Chem 278, 20405–20412.
Liu D, Vleugel M, Backer CB, Hori T, Fukagawa T, Cheeseman IM, Lampson MA (2010). Regulated targeting of protein phosphatase 1 to the outer kinetochore by KNL1 opposes Aurora B kinase. J Cell Biol 188, 809–820.
London N, Ceto S, Ranish JA, Biggins S (2012). Phosphoregulation of Spc105 by Mps1 and PP1 regulates Bub1 localization to kinetochores. Curr Biol 22, 900–906.
Luo J, Deng X, Buehl C, Xu X, Kuo MH (2016). Identification of tension sensing motif of histone H3 in *Saccharomyces cerevisiae* and its regulation by histone modifying enzymes. Genetics 204, 1029–1043.
Luo J, Xu X, Hall H, Hyland EM, Boeke JD, Hazbun T, Kuo MH (2010). Histone H3 exerts a key function in mitotic checkpoint control. Mol Cell Biol 30, 537–549.
Mason AG, Garza RM, McCormick MA, Patel B, Kennedy BK, Pillus L, La Spada AR (2017). The replicative lifespan-extending deletion of *SGF73* results in altered ribosomal gene expression in yeast. Aging Cell 16, 785–796.
McKinley KL, Cheeseman IM (2016). The molecular basis for centromere identity and function. Nat Rev Mol Cell Biol 17, 16–29.
Meluh PB, Yang P, Glowczewski L, Koshland D, Smith MM (1998). Cse4p is a component of the core centromere of *Saccharomyces cerevisiae*. Cell 94, 607–613.
Mishra PK, Thapa KS, Chen P, Wang S, Hazbun TR, Basrai MA (2017). Budding yeast CENP-A/Cse4 interacts with the N-terminus of Sgo1 and regulates its association with centromeric chromatin. Cell Cycle 17, 11–23.
Morey L, Barnes K, Chen Y, Fitzgerald-Hayes M, Baker RE (2004). The histone fold domain of Cse4 is sufficient for CEN targeting and propagation of active centromeres in budding yeast. Eukaryot Cell 3, 1533–1543.
Nasa I, Kettenbach AN (2018). Coordination of protein kinase and phosphoprotein phosphatase activities in mitosis. Front Cell Dev Biol 6, 30.
Nerusheva OO, Galander S, Fernius J, Kelly D, Marston AL (2014). Tension-dependent removal of pericentromeric shugoshin is an indicator of sister chromosome biorientation. Genes Dev 28, 1291–1309.
Ng TM, Lenstra TL, Duggan N, Jiang S, Ceto S, Holstege FC, Dai J, Boeke JD, Biggins S (2013). Kinetochore function and chromosome segregation rely on critical residues in histones H3 and H4 in budding yeast. Genetics 195, 795–807.
Ohkuni K, Levy-Myers R, Warren J, Au WC, Takahashi Y, Baker RE, Basrai MA (2018). N-terminal sumoylation of centromeric histone H3 variant Cse4 regulates its proteolysis to prevent mislocalization to non-centromeric chromatin. G3 (Bethesda) 8, 1215–1223.
Ohkuni K, Takahashi Y, Fulp A, Lawrimore J, Au WC, Pasupala N, Levy-Myers R, Warren J, Strunnikov A, Baker RE, *et al*. (2016). SUMO-targeted ubiquitin ligase (STUbL) Slx5 regulates proteolysis of centromeric histone H3 variant Cse4 and prevents its mislocalization to euchromatin. Mol Biol Cell 27, 1409–1551.
Onn I, Heidinger-Pauli JM, Guacci V, Unal E, Koshland DE (2008). Sister chromatid cohesion: a simple concept with a complex reality. Annu Rev Cell Dev Biol 24, 105–129.
Ouspenski II, Elledge SJ, Brinkley BR (1999). New yeast genes important for chromosome integrity and segregation identified by dosage effects on genome stability. Nucleic Acids Res 27, 3001–3008.
Patel JH, Du Y, Ard PG, Phillips C, Carella B, Chen CJ, Rakowski C, Chatterjee C, Lieberman PM, Lane WS, *et al*. (2004). The c-MYC oncoprotein is a substrate of the acetyltransferases hGCN5/PCAF and TIP60. Mol Cell Biol 24, 10826–10834.
Peplowska K, Wallek AU, Storchova Z (2014). Sgo1 regulates both condensin and Ipl1/Aurora B to promote chromosome biorientation. PLoS Genet 10, e1004411.
Petty EL, Lafon A, Tomlinson SL, Mendelsohn BA, Pillus L (2016). Promotion of cell viability and histone gene expression by the acetyltransferase Gcn5 and the protein phosphatase PP2A in *Saccharomyces cerevisiae*. Genetics 203, 1693–1707.
Popsel J (2015). Characterization of a Novel Lysine Acetylation Site in the N-Terminal Domain of the Centromeric Histone Variant Cse4 in *Saccharyomyces cerevisiae*. Doctoral Thesis. Lebenswissenschaftliche Fakultät, Humboldt-Universität zu Berlin, pp. 126, https://edoc.hu-berlin.de/handle/18452/17995 (accessed 6 January 2018).
Pray-Grant MG, Schieltz D, McMahon SJ, Wood JM, Kennedy EL, Cook RG, Workman JL, Yates JR 3rd, Grant PA (2002). The novel SLIK histone acetyltransferase complex functions in the yeast retrograde response pathway. Mol Cell Biol 22, 8774–8786.
Primorac I, Weir JR, Chiroli E, Gross F, Hoffmann I, van Gerwen S, Ciliberto A, Musacchio A (2013). Bub3 reads phosphorylated MELT repeats to promote spindle assembly checkpoint signaling. Elife 2, e01030.
Ranjitkar P, Press MO, Yi X, Baker R, MacCoss MJ, Biggins S (2010). An E3 ubiquitin ligase prevents ectopic localization of the centromeric histone H3 variant via the centromere targeting domain. Mol Cell 40, 455–464.
Riedel CG, Katis VL, Katou Y, Mori S, Itoh T, Helmhart W, Galova M, Petronczki M, Gregan J, Cetin B, *et al*. (2006). Protein phosphatase 2A protects centromeric sister chromatid cohesion during meiosis I. Nature 441, 53–61.
Roberts SM, Winston F (1997). Essential functional interactions of SAGA, a *Saccharomyces cerevisiae* complex of Spt, Ada, and Gcn5 proteins, with the Snf/Swi and Srb/mediator complexes. Genetics 147, 451–465.
Rosaleny LE, Ruiz-Garcia AB, Garcia-Martinez J, Perez-Ortin JE, Tordera V (2007). The Sas3p and Gcn5p histone acetyltransferases are recruited to similar genes. Genome Biol 8, R119.
Rose MD, Winston FM, Hieter P (1990). Methods in Yeast Genetics: A Laboratory Course Manual, Cold Spring Harbor, NY.: Cold Spring Harbor Laboratory Press.
Samel A, Cuomo A, Bonaldi T, Ehrenhofer-Murray AE (2012). Methylation of CenH3 arginine 37 regulates kinetochore integrity and chromosome segregation. Proc Natl Acad Sci USA 109, 9029–9034.
Schneider CA, Rasband WS, Eliceiri KW (2012). NIH Image to ImageJ: 25 years of image analysis. Nat Methods 9, 671–675.
Shepperd LA, Meadows JC, Sochaj AM, Lancaster TC, Zou J, Buttrick GJ, Rappsilber J, Hardwick KG, Millar JB (2012). Phosphodependent recruitment of Bub1 and Bub3 to Spc7/KNL1 by Mph1 kinase maintains the spindle checkpoint. Curr Biol 22, 891–899.
Shrestha RL, Ahn GS, Staples MI, Sathyan KM, Karpova TS, Foltz DR, Basrai MA (2017). Mislocalization of centromeric histone H3 variant CENP-A contributes to chromosomal instability (CIN) in human cells. Oncotarget 8, 46781–46800.
Sterner DE, Belotserkovskaya R, Berger SL (2002). SALSA, a variant of yeast SAGA, contains truncated Spt7, which correlates with activated transcription. Proc Natl Acad Sci USA 99, 11622–11627.
Stirling PC, Bloom MS, Solanki-Patil T, Smith S, Sipahimalani P, Li Z, Kofoed M, Ben-Aroya S, Myung K, Hieter P (2011). The complete spectrum of yeast chromosome instability genes identifies candidate CIN cancer genes and functional roles for ASTRA complex components. PLoS Genet 7, e1002057.
Stoler S, Keith KC, Curnick KE, Fitzgerald-Hayes M (1995). A mutation in *CSE4*, an essential gene encoding a novel chromatin-associated protein in yeast, causes chromosome nondisjunction and cell cycle arrest at mitosis. Genes Dev 9, 573–586.
Strickfaden SC, Winters MJ, Ben-Ari G, Lamson RE, Tyers M, Pryciak PM (2007). A mechanism for cell-cycle regulation of MAP kinase signaling in a yeast differentiation pathway. Cell 128, 519–531.
Sun X, Clermont PL, Jiao W, Helgason CD, Gout PW, Wang Y, Qu S (2016). Elevated expression of the centromere protein-A(CENP-A)-encoding gene as a prognostic and predictive biomarker in human cancers. Int J Cancer 139, 899–907.
Tessarz P, Kouzarides T (2014). Histone core modifications regulating nucleosome structure and dynamics. Nat Rev Mol Cell Biol 15, 703–708.
Theis JF, Irene C, Dershowitz A, Brost RL, Tobin ML, di Sanzo FM, Wang JY, Boone C, Newlon CS (2010). The DNA damage response pathway contributes to the stability of chromosome III derivatives lacking efficient replicators. PLoS Genet 6, e1001227.
Thompson JD, Higgins DG, Gibson TJ (1994). CLUSTAL W: improving the sensitivity of progressive multiple sequence alignment through sequence weighting, position-specific gap penalties and weight matrix choice. Nucleic Acids Res 22, 4673–4680.
Torres-Machorro AL, Aris JP, Pillus L (2015). A moonlighting metabolic protein influences repair at DNA double-stranded breaks. Nucleic Acids Res 43, 1646–1658.
Vernarecci S, Ornaghi P, Bagu A, Cundari E, Ballario P, Filetici P (2008). Gcn5p plays an important role in centromere kinetochore function in budding yeast. Mol Cell Biol 28, 988–996.
Verzijlbergen KF, Nerusheva OO, Kelly D, Kerr A, Clift D, de Lima Alves F, Rappsilber J, Marston AL (2014). Shugoshin biases chromosomes for biorientation through condensin recruitment to the pericentromere. eLife 3, e01374.
Wang L, Dent SY (2014). Functions of SAGA in development and disease. Epigenomics 6, 329–339.

Wang L, Liu L, Berger SL (1998). Critical residues for histone acetylation by Gcn5, functioning in Ada and SAGA complexes, are also required for transcriptional function in vivo. Genes Dev 12, 640–653.

Wang Y, Burke DJ (1995). Checkpoint genes required to delay cell division in response to nocodazole respond to impaired kinetochore function in the yeast *Saccharomyces cerevisiae*. Mol Cell Biol 15, 6838–6844.

Xu Z, Cetin B, Anger M, Cho US, Helmhart W, Nasmyth K, Xu W (2009). Structure and function of the PP2A-shugoshin interaction. Mol Cell 35, 426–441.

Yamagishi Y, Yang CH, Tanno Y, Watanabe Y (2012). MPS1/Mph1 phosphorylates the kinetochore protein KNL1/Spc7 to recruit SAC components. Nat Cell Biol 14, 746–752.

Yu HG, Koshland D (2007). The Aurora kinase Ipl1 maintains the centromeric localization of PP2A to protect cohesin during meiosis. J Cell Biol 176, 911–918.

Zapata J, Dephoure N, Macdonough T, Yu Y, Parnell EJ, Mooring M, Gygi SP, Stillman DJ, Kellogg DR (2014). PP2A-Rts1 is a master regulator of pathways that control cell size. J Cell Biol 204, 359–376.

Zhang W, Bone JR, Edmondson DG, Turner BM, Roth SY (1998). Essential and redundant functions of histone acetylation revealed by mutation of target lysines and loss of the Gcn5p acetyltransferase. EMBO J 17, 3155–3167.

Zhao Y, Boguslawski G, Zitomer RS, DePaoli-Roach AA (1997). *Saccharomyces cerevisiae* homologs of mammalian B and B′ subunits of protein phosphatase 2A direct the enzyme to distinct cellular functions. J Biol Chem 272, 8256–8262.

Zhou Z, Feng H, Zhou BR, Ghirlando R, Hu K, Zwolak A, Miller Jenkins LM, Xiao H, Tjandra N, Wu C, *et al.* (2011). Structural basis for recognition of centromere histone variant CenH3 by the chaperone Scm3. Nature 472, 234–237.

Supplemental Materials

Molecular Biology of the Cell

Petty et al.

Supplemental Figure Legends

FIGURE S1. Steady state expression of *CSE4*, *RTS1*, and *SGO1* is unchanged in *gcn5*Δ*.* RNA was extracted from logarithmically growing wild-type and gcn5Δ cells and expression determined by RT-qPCR. As expected, the negative control gene *ADH1* gene showed no significant change in expression, whereas expression of the positive control *CWP1*, was significantly decreased upon loss of Gcn5. Loss of *gcn5*Δ did not significantly alter steady-state expression of *CSE4*, *RTS1* or *SGO1*. Shown are average expression levels relative to *SCR1*, a well-established *GCN5*-independent gene control, from three independent experiments; error bars indicate standard deviation.

FIGURE S2. A view of SAGA subunits detected near centromeres in established genome-binding studies. Chromatin endogenous cleavage sequencing (ChEC-seq) binding data of Spt7, Spt8, and Ubp8 (Baptista et al., 2017) and ChIP-seq data of Sgf73 (Mason et al., 2017) and Cse4 (Hildebrand & Biggins, 2016) were visualized using IGV_2.3.92 (Robinson, Thorvaldsdottir et al., 2011, Thorvaldsdottir, Robinson et al., 2013). The ChIII:112,899-116,297 window including CenIII is shown above and the ChIV: 447,942-452,052 window including CenIV is shown below. SAGA Spt module subunit profiles are in blue, SAGA DUB module subunit profiles are in purple, and the Cse4 profile is shown in red.

FIGURE S3. Rts1-3PK is expressed in *sgo1-N51I* cells, and HA-cse4 is expressed in all strains used for analysis. (A) Freshly transformed strains bearing a single, integrated copy of *RTS1-3PK* or with the additional *RTS1-3PK* 2μM plasmid were grown to log

phase for protein lysate preparation and detected by anti-V5 immunoblot. (B) Lysate was prepared from logarithmically growing HA-cse4 strains freshly transformed with either 2μM-vector or 2μM-*RTS1* and Cse4 expression detected by anti-HA immunoblot. Lysates were analyzed from four sets of transformants; shown are representative images of one experimental transformant set.

FIGURE S4.The *cse4-K215R* mutation causes temperature and nocodazole sensitivity in *GCN5* cells that is alleviated by acetyl-mimetic *cse4-K215Q* mutation. Transformants were grown overnight, normalized, and five-fold serial dilutions were plated onto control (URA- and YPAD) and challenge plates (pre-warmed to 37˚ and 2μM nocodazole). Images were collected at Day 3. Shown is an image set representative of four independent experiments.

FIGURE S5. Rts1-3PK ChIP in *GCN5 cse4-S180* mutants. Metaphase-arrested *GCN5* transformants were fixed and analyzed for Rts1 binding at the centromere by ChIP-qPCR. Shown are average percent input values of three independent experiments; error bars indicate standard deviation.

FIGURE S6. Relative HA-Cse4 and Rts1-3PK levels in *CSE4* and *cse4-S180* mutant strains. Protein lysate was prepared from log-phase transformants bearing a single, integrated copy of *RTS1-3PK* or with the additional *RTS1-3PK* 2μM plasmid. (A) Representative immunoblots from wild-type and *gcn5*Δ transformants are shown. (B) Levels of HA-Cse4 and Rts1-3PK were determined relative to tubulin by ImageJ

analysis of immunoblots from four independent experiments. In general, overexpression of *RTS1* led to increases in Cse4 levels. HA-cse4-S180A has lower abundance in both *GCN5* and *gcn5*Δ backgrounds, whereas HA-cse4-S180E abundance is lower only in *gcn5*Δ. Rts1-3PK expression and overexpression remained consistent in all strains.

FIGURE S7. Confirmation of HA-cse4-S180EE expression in *cse4*Δ/+ diploid cells. Protein lysate was prepared from log-phase transformants bearing a single chromosomal copy of *CSE4* as well as the *TRP1*-marked CEN plasmid with *CSE4* or *cse4-S180EE*. (A) Representative immunoblot from four independent diploid transformants per plasmid are shown. (B) Levels of HA-Cse4 were determined relative to tubulin by ImageJ analysis.

Figure S1.

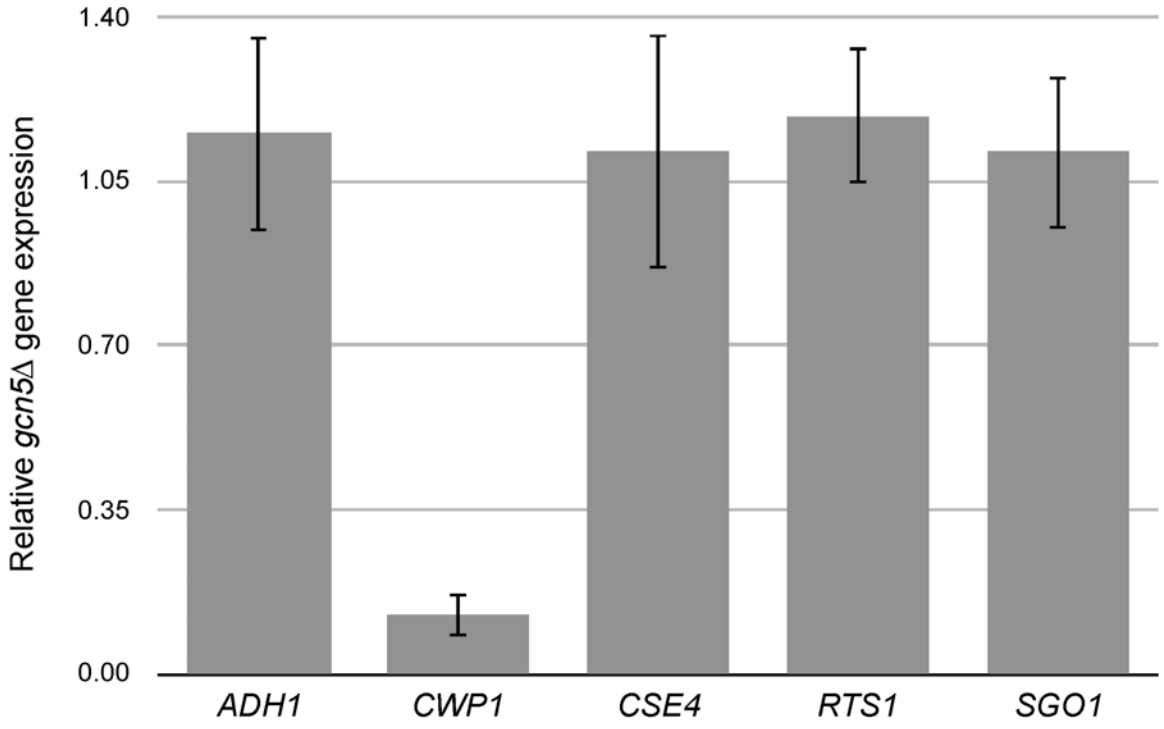
1.40
1.05
0.70
0.35
0.00
Relative gcn5Δ gene expression
ADH1
CWP1
CSE4
RTS1
SGO1

Figure S2.

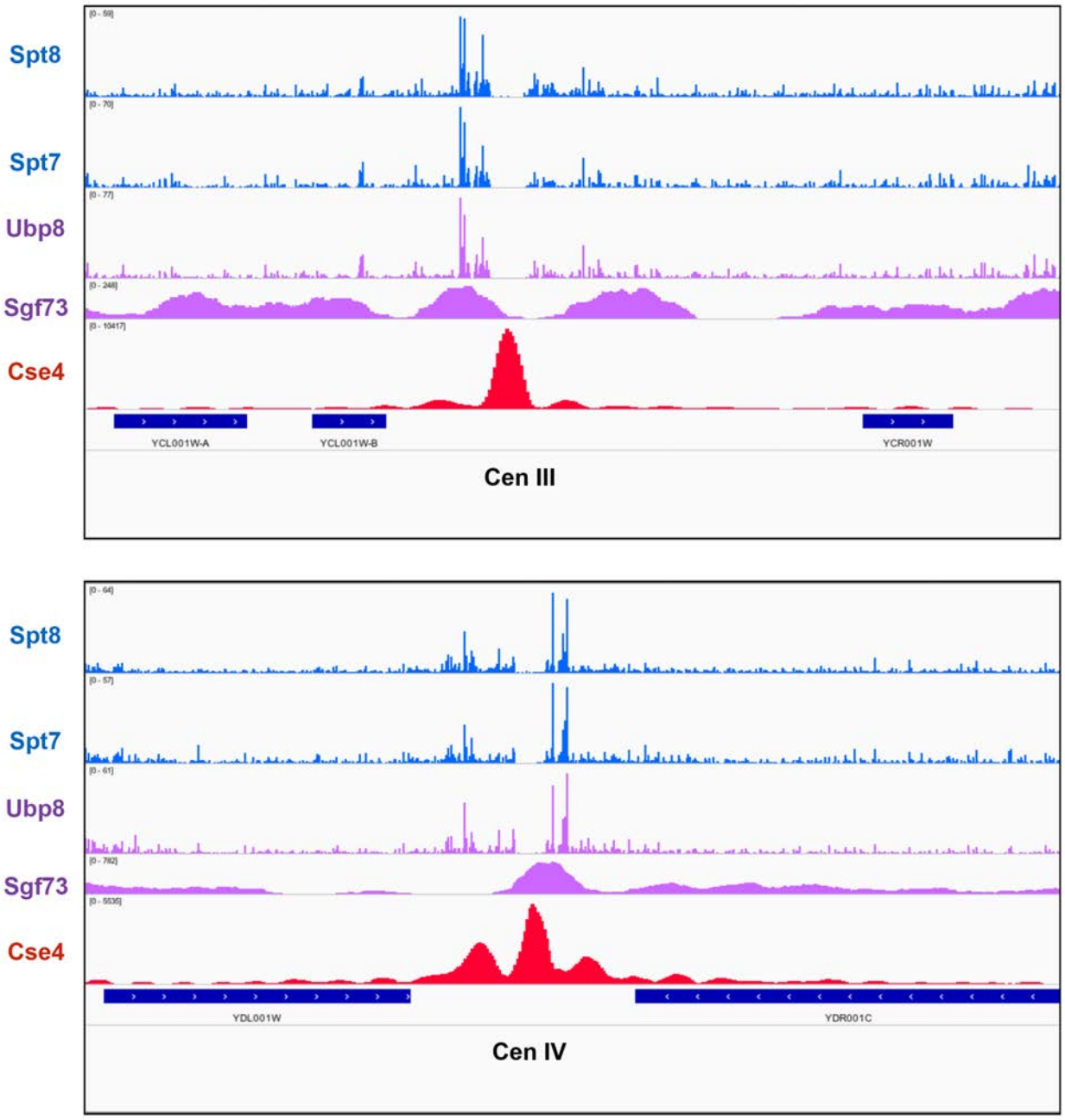
Spt8
Spt7
Ubp8
Sgf73
Cse4
YCL001W-A
YCL001W-B
YCR001W
Cen III
Spt8
Spt7
Ubp8
Sgf73
Cse4
YDL001W
YDR001C
Cen IV

Figure S3.

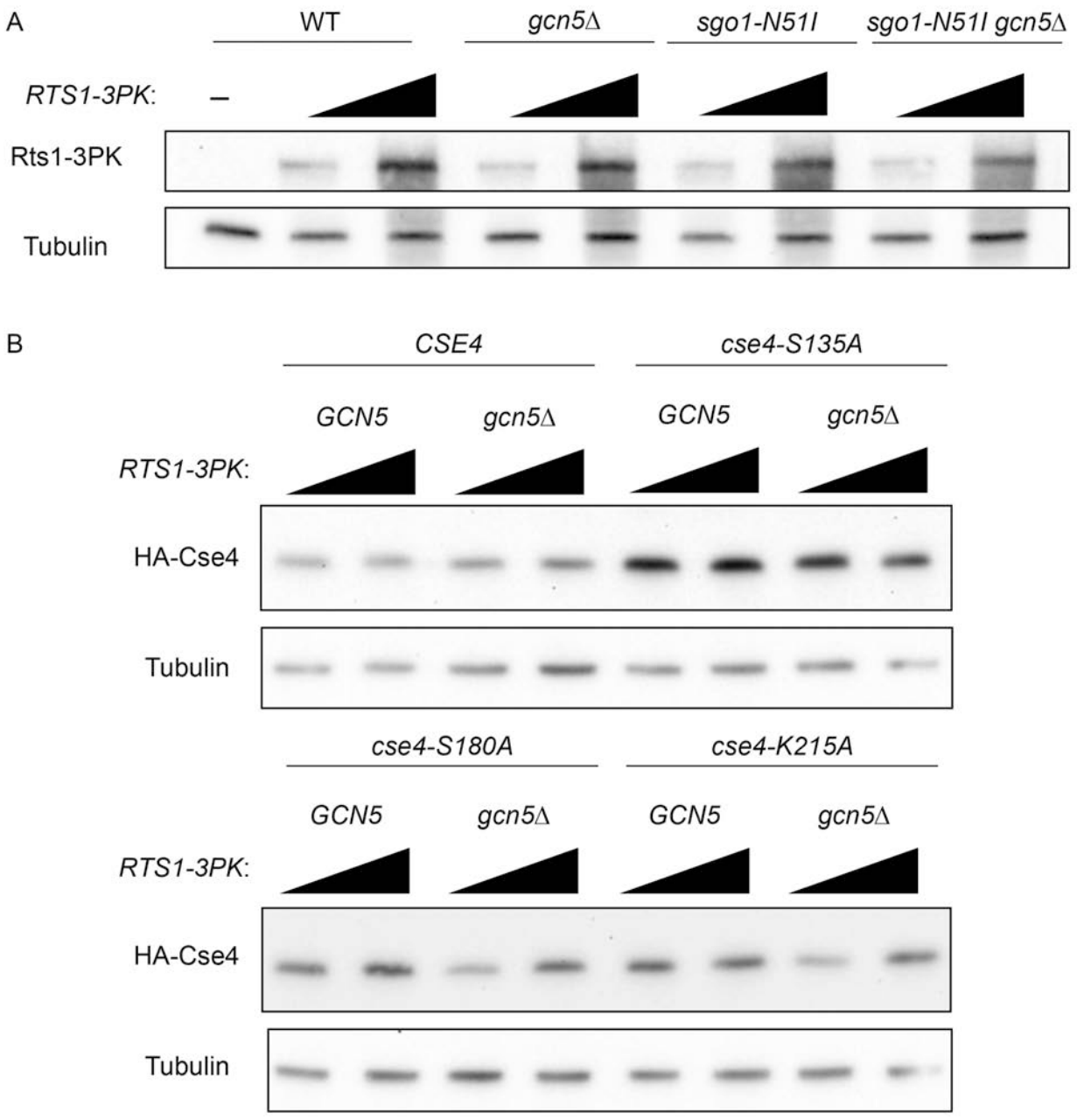
A
WT
gcn5Δ
sgo1-N51I
sgo1-N51I gcn5Δ
RTS1-3PK:
–
Rts1-3PK
Tubulin
B
CSE4
cse4-S135A
GCN5
gcn5Δ
GCN5
gcn5Δ
RTS1-3PK:
HA-Cse4
Tubulin
cse4-S180A
cse4-K215A
GCN5
gcn5Δ
GCN5
gcn5Δ
RTS1-3PK:
HA-Cse4
Tubulin

Figure S4.

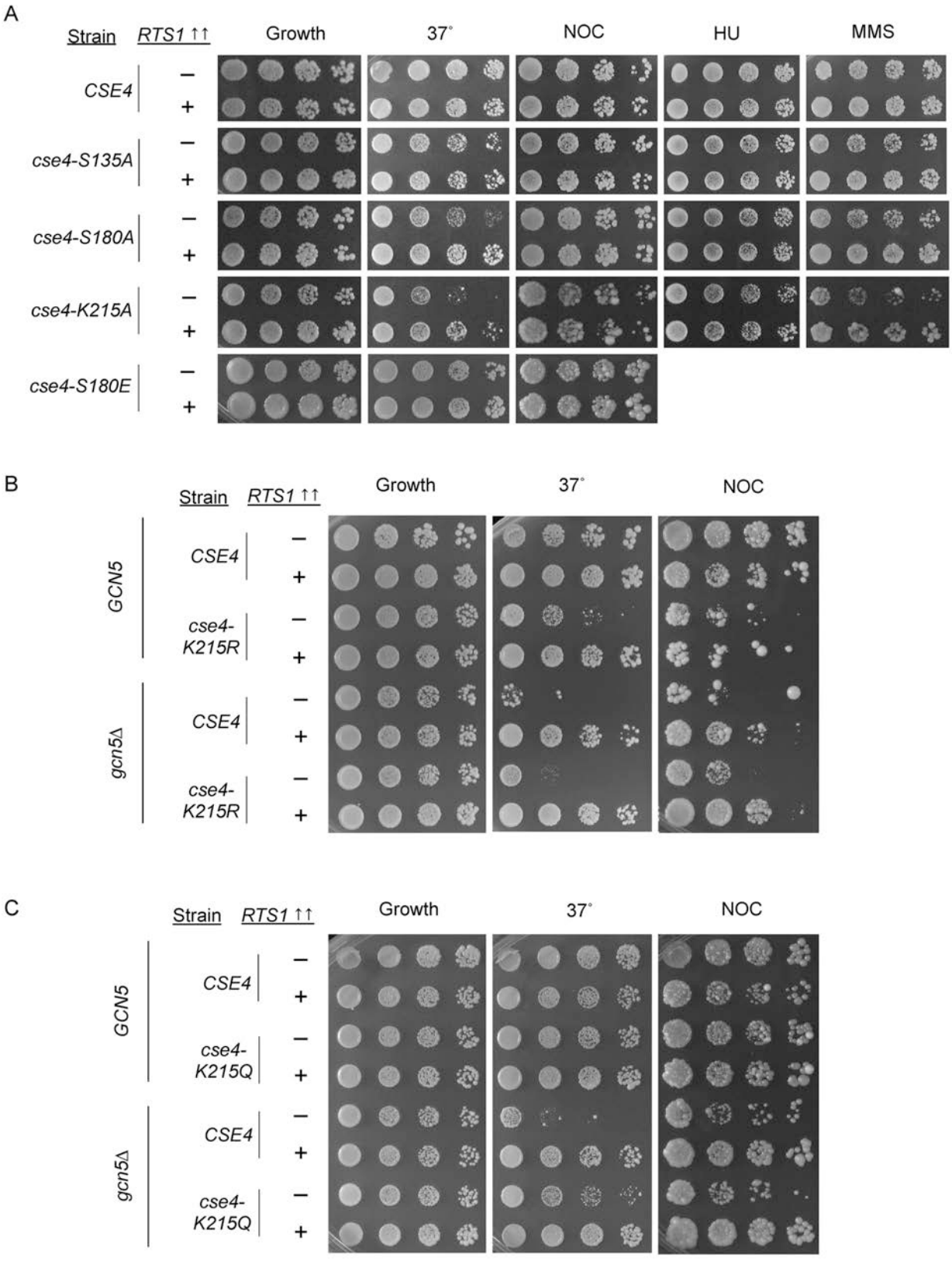
A
Strain
RTS1 ↑↑
Growth
37°
NOC
HU
MMS
CSE4
cse4-S135A
cse4-S180A
cse4-K215A
cse4-S180E
B
Strain
RTS1 ↑↑
Growth
37°
NOC
GCN5
gcn5Δ
CSE4
cse4-K215R
C
Strain
RTS1 ↑↑
Growth
37°
NOC
GCN5
gcn5Δ
CSE4
cse4-K215Q

Figure S5.

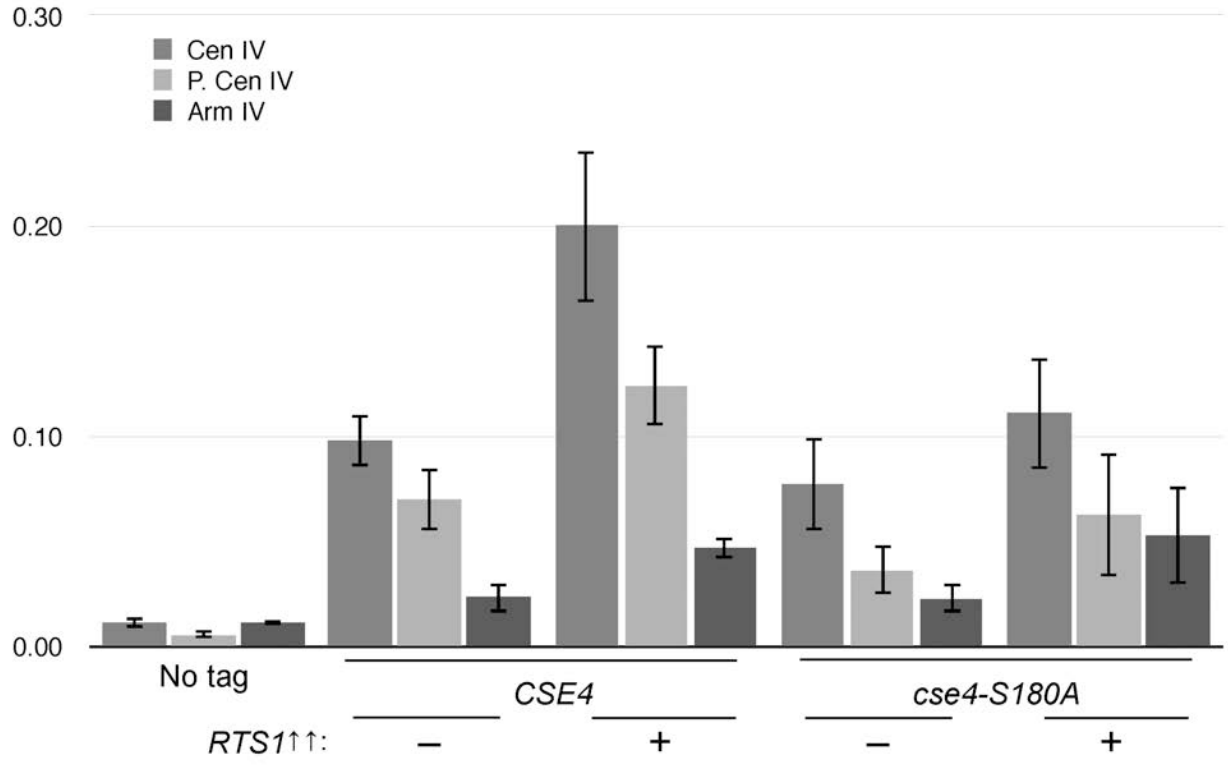
0.30
0.20
0.10
0.00
Cen IV
P. Cen IV
Arm IV
No tag
CSE4
cse4-S180A
RTS1↑↑:
–
+
–
+

Figure S6.

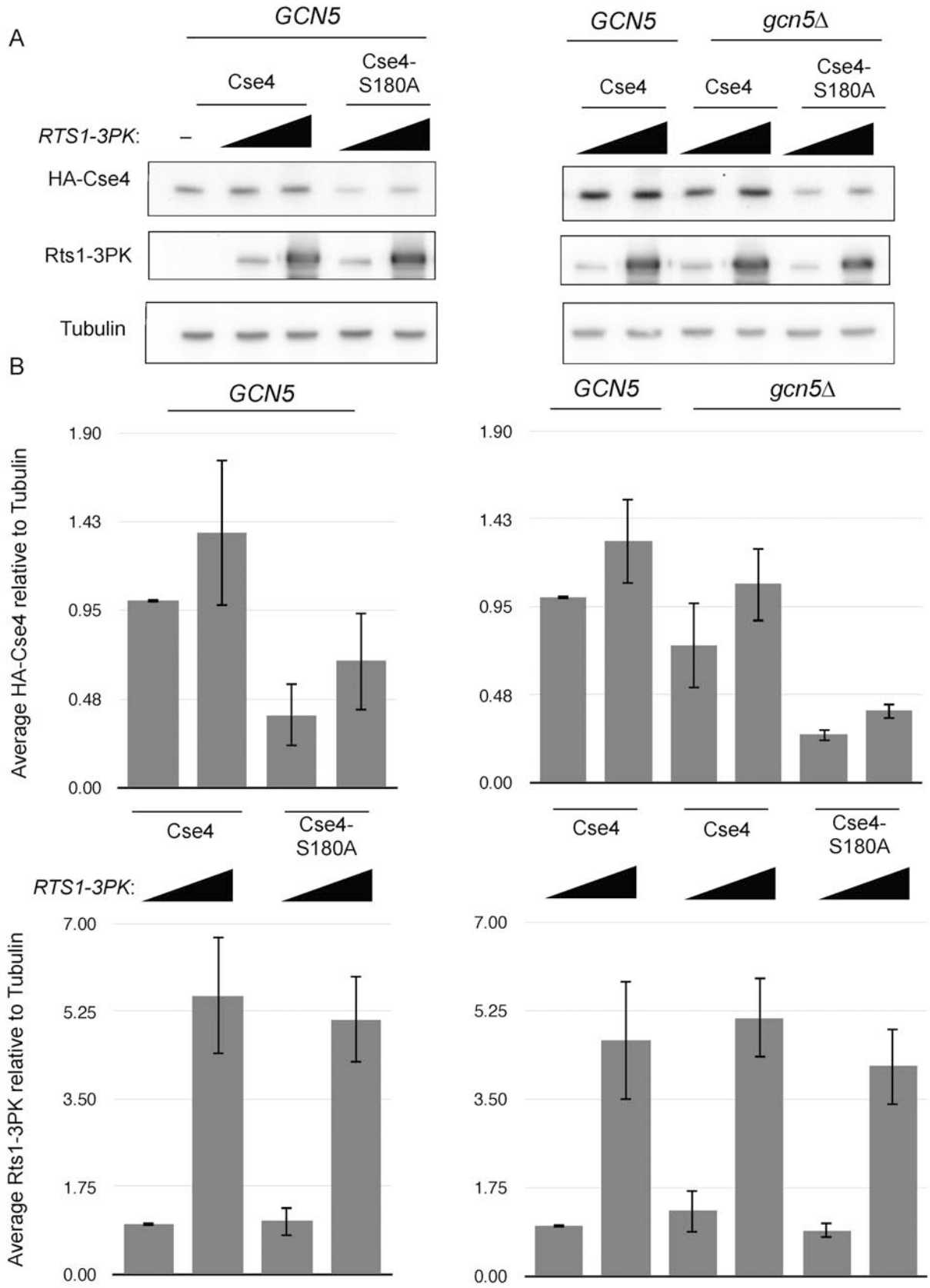
A
GCN5
GCN5
gcn5Δ
Cse4
Cse4-S180A
Cse4
Cse4
Cse4-S180A
RTS1-3PK:
–
HA-Cse4
Rts1-3PK
Tubulin
B
GCN5
GCN5
gcn5Δ
Average HA-Cse4 relative to Tubulin
1.90
1.43
0.95
0.48
0.00
Cse4
Cse4-S180A
Cse4
Cse4
Cse4-S180A
RTS1-3PK:
Average Rts1-3PK relative to Tubulin
7.00
5.25
3.50
1.75
0.00

Figure S7.

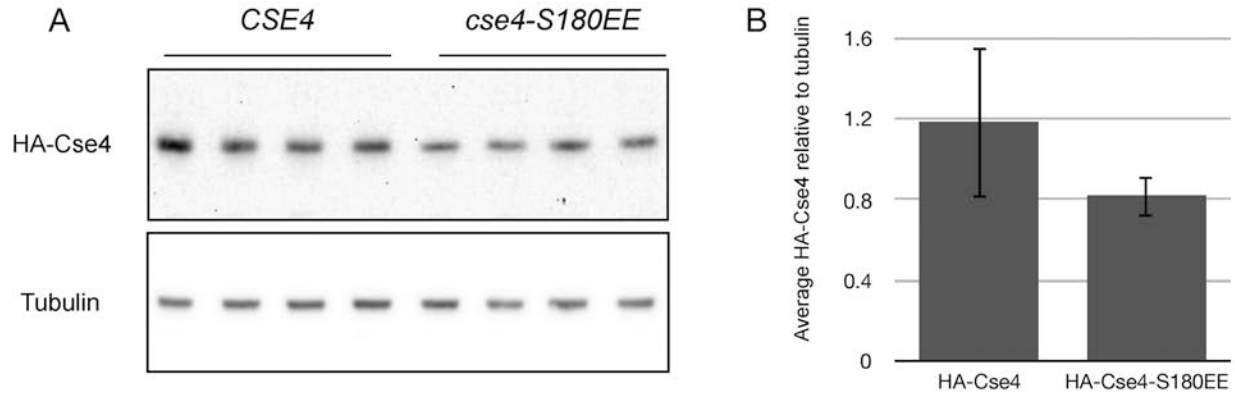
A
CSE4
cse4-S180EE
HA-Cse4
Tubulin
B
Average HA-Cse4 relative to tubulin
1.6
1.2
0.8
0.4
0
HA-Cse4
HA-Cse4-S180EE